ORNL/TM-2020/1713

Nuclear Criticality Safety Assessment of Criticality Control Containers without Moderation Control at the Waste Isolation Pilot Plant

Ellen M. Saylor

September 2020

Approved for public release.
Distribution is unlimited.

OAK RIDGE NATIONAL LABORATORY
MANAGED BY UT-BATTELLE FOR THE US DEPARTMENT OF ENERGY

ORNL/TM-2020/1713

Reactor and Nuclear Systems Division

NUCLEAR CRITICALITY SAFETY ASSESSMENT OF CRITICALITY CONTROL CONTAINERS WITHOUT MODERATION CONTROL AT THE WASTE ISOLATION PILOT PLANT

Ellen M. Saylor

September 2020

Prepared by
OAK RIDGE NATIONAL LABORATORY
Oak Ridge, TN 37831-6283
managed by
UT-BATTELLE, LLC
for the
US DEPARTMENT OF ENERGY
under contract DE-AC05-00OR22725

REVISION LOG

Revision	Sections changed	Description of change	Date
0	N/A	Initial issue	September 2020

CONTENTS

LIST OF FIGURES

LIST OF TABLES

ACRONYMS

ANSI	American National Standards Institute
CBFO	Carlsbad Field Office
CCA	Compliance Certification Application
CCC	criticality control container
CCO	criticality control overpack
CH-TRAMPAC	Contact-Handled Transuranic Waste Authorized Methods for Payload Control
CSAS	criticality safety analysis sequence
DC	degraded configuration
DOE	US Department of Energy
DWG	drawing
EALF	energy of average neutron lethargy causing fission
EPA	US Environmental Protection Agency
FEP	feature, event, and process
FGE	fissile gram equivalent
HalfPACT	Half-Package Transporter
IHECSBE	*International Handbook of Evaluated Criticality Safety Benchmark Experiments*
MCNP	Monte Carlo N-Particle code
MCT	mixed composition thermal
MOX	mixed oxide
MST	mixed solution thermal
NEA	Nuclear Energy Agency
NF	nonfissionable
NM	New Mexico
NPS	nominal pipe size
NWP	Nuclear Waste Partnership, LLC
ORNL	Oak Ridge National Laboratory
POC	pipe overpack container
PST	plutonium solution thermal
RNSD	Reactor and Nuclear Systems Division
SBMS	Systems-Based Management System
SCALE	Standardized Computer Analysis for Licensing Evaluation
SNL	Sandia National Laboratory
SPC	specification
SS	stainless steel
S/U	sensitivity/uncertainty
TRU	transuranic
TRUPACT	TRU Package Transporter
USL	upper subcritical limit
USLSTATS	Upper Subcritical Limit Statistics
WIPP	Waste Isolation Pilot Plant

EXECUTIVE SUMMARY

The Waste Isolation Pilot Plant (WIPP) provides for safe, permanent disposal of government-owned transuranic (TRU) and TRU mixed wastes. Receipt and disposal of waste at the WIPP site began in March 1999. The Sandia report, *Consideration of Nuclear Criticality When Disposing of Transuranic Waste at the Waste Isolation Pilot Plant*, addressed potential nuclear criticality safety issues based on the projected inventory characteristics known at the time [1]. As designs for inventory, waste forms, and disposal packages have changed, new analyses have been performed, and updates have been made to address any potential effects to the WIPP safety basis.

New analyses performed include Saylor 2017 [2] and Brickner 2019 [3], which address certain waste containers with specified loadings under post-closure conditions. Both examined several hypothetical scenarios and included analyses to bound (from a criticality potential standpoint) credible configurations that could occur at WIPP during the repository regulatory post-closure disposal time period for feature, event, and process (FEP) considerations—10,000 years. During this post-closure period at WIPP, the screening of FEPs is governed by the risk-based standards and implementing regulations of the US Environmental Protection Agency (EPA) (i.e., 40 CFR 191 and 40 CFR 194, respectively) [4,5]. An FEP screening can be based on either a low-consequence or low-probability rationale. A low-probability rationale includes either (a) a qualitative rationale that the FEP is not credible or (b) a quantitative demonstration that the probability is less than 10^{-4} in 10^{4} years. In this evaluation, a qualitative low-probability rationale of *not credible* is used by demonstrating that bounding configurations of the waste are not critical. The demonstration of subcriticality is through quantitative calculations, but a probability of criticality is not evaluated. Rather, the rationale for this evaluation is that bounding configurations with an effective neutron multiplication factor (k_{eff}) well below the upper subcriticality limit (USL) make criticality incredible.

Reference [2] documented a nuclear criticality assessment of the WIPP repository for disposal of dilute surplus plutonium materials using the Dilute and Dispose Approach and packaging in criticality control overpacks (CCOs). The CCO is the waste disposal container recently designed to allow for up to 380 fissile gram equivalent (FGE) ^{239}Pu per drum, which is a higher fissile loading than typical waste containers. The CCO consists of a criticality control container (CCC) positioned by upper and lower plywood spacers within a standard 55 gal drum. The CCC is used to establish a geometry control for fissile materials during transportation and WIPP emplacement operations. The current WIPP waste acceptance criteria for CCO payloads limit beryllium to less than or equal to 1% by weight of the waste contents and require the waste form to be non-machine compacted.

Reference [2] considered two scenario progressions—room closure from salt creep, hereafter referred to as the *reconfigured dry* scenario, and flooding with brine, hereafter referred to as the *reconfigured wet* scenario. The subsequent drying out of the reconfigured wet scenarios was also considered. For all scenarios, subcriticality was maintained when 50 g of B_4C (acting as a neutron absorber) per CCC was intermixed within the plutonium disposition waste form. The analysis used a waste form description that limits the amount of moderation that could be present within the waste form (i.e., it limits the amount of water and polyethylene that could be present based on planned processing conditions).

This analysis to evaluate increased limits on the amount of moderation that could be present was performed as a companion to Reference [2] to address concerns associated with verifying moisture and/or plastic contents of waste materials following packaging of dilute surplus plutonium in the CCO. To that end, this analysis used the models and methods from Reference [2] to evaluate a more generic base waste form consisting of water and polyethylene that is more similar (and nearly identical) to the generic waste forms utilized in other models/analyses supporting the TRU Package Transporter Model II (TRUPACT-II) safety analysis [6] (all are without moderation controls). The waste form in this analysis uses a base

mixture of 75% water and 25% polyethylene, the total amount of which is varied to determine the optimum moderation to fissile material (H/Pu) ratio. The fissile loading is maintained at up to 380 FGE ^{239}Pu (modeled as PuO_2) per CCO with an additional 545 g of beryllium (to bound the 1% by weight contents restriction) and 50 g of B_4C intermixed per CCO. The beryllium content (1% by weight) is based on the total allowed waste weight (this does not include packaging and container weights).

Figures ES-1 and ES-2 display summary results, showing that with this model including 50 g of B_4C per CCO, the system k_{eff} remains under 0.85 for all moderator amounts and provides a significant margin against post-closure criticality under postulated bounding conditions for compaction. Figure ES-1 compares an infinite model with a room model at the initial emplacement spacing and under full radial compaction. Full radial compaction places each CCC in direct contact and does not credit any anticipated spacing associated with current post-closure geomechanical modeling of the repository [7]. The effects of variations in the H/Pu ratio were evaluated by varying the amount of the water/polyethylene component of the waste model, with fissile loading maintained at 380 ^{239}Pu FGE. Similarly, Figure ES-2 illustrates how various amounts of B_4C per CCO influence k_{eff} at different radial compactions, all at the H/Pu ratio of 200 (in the room array model). Therefore, while the results from Saylor 2017 [2] modeled more realistic process limits associated with packaging of dilute surplus plutonium, this analysis demonstrates that limits on moderation (plastic and water content) are not necessary to ensure subcriticality in the WIPP repository, provided the requisite B_4C absorber is present.

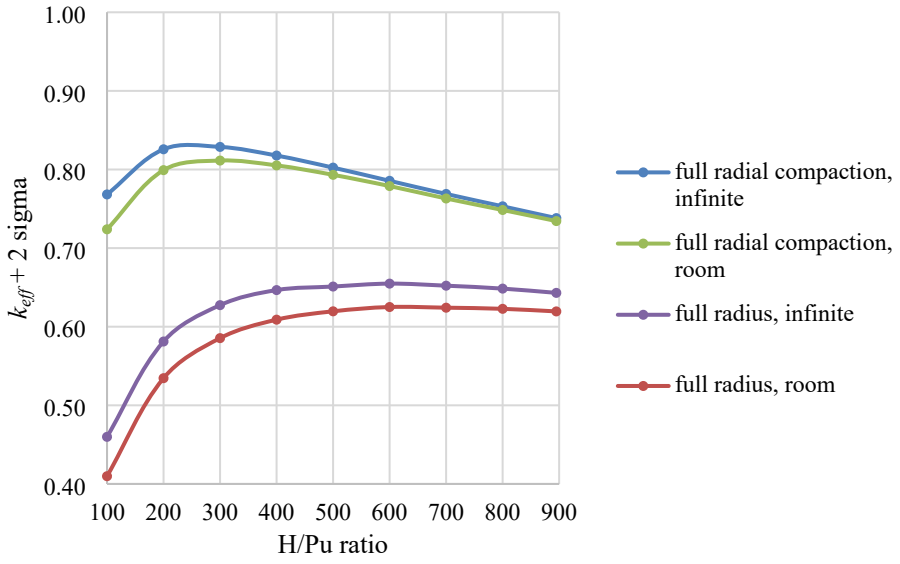

Figure ES-1. System k_{eff} as a function of the H/Pu ratio with 50 g of B_4C per CCO.

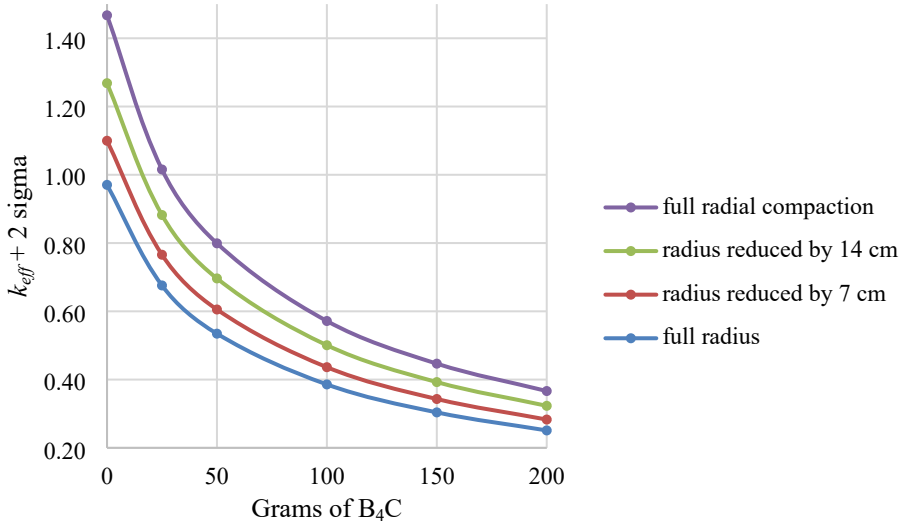

Figure ES-2. Results for incorporating B_4C into the fissile material mixture (H/Pu of 200).

REFERENCES

[1] R. Rechard, L. Sanchez, C. Stockman, Holly T. 2000. *Consideration of Nuclear Criticality When Disposing of Transuranic Waste at the Waste Isolation Pilot Plant,* SAND99-2898, Sandia National Laboratories, Albuquerque, New Mexico.

[2] E. M. Saylor. 2017, *Nuclear Criticality Safety Assessment of Potential Disposition at the Waste Isolation Plant*, ORNL/TM-2017/751/R1, Oak Ridge National Laboratory, Oak Ridge, Tennessee.

[3] B. Brickner. 2019. *Post Placement Nuclear Criticality Evaluations Involving 6- and 12-Inch Pipe Overpack TRU Waste Containers at the Waste Isolation Pilot Plant*, ORNL/TM-2019/1222/R0, Oak Ridge National Laboratory, Oak Ridge, Tennessee.

[4] EPA (U.S. Environmental Protection Agency). 1993. 40 CFR Part 191: *Environmental Radiation Protection Standards for Management and Disposal of Spent Nuclear Fuel, High-Level and Transuranic Radioactive Wastes; Final Rule*, *Federal Register*. Vol 58, no. 242, 66398-66416.

[5] EPA (U.S. Environmental Protection Agency). 1996. 40 CFR Part 194: *Criteria for the Certification and Recertification of the Waste Isolation Pilot Plant's Compliance with the 40 CFR Part 191 Disposal Regulations; Final Rule*, *Federal Register*. Vol 61, no. 28, 5224-5245.

[6] DOE-CBFO. 2013. *TRUPACT-II Safety Analysis Report*, Revision 23, US Department of Energy, Carlsbad Field Office, Carlsbad, New Mexico.

[7] B. Reedlunn and J. Bean. 2020. *Further Simulations of Criticality Control Overpack Container Compaction at the Waste Isolation Pilot Plant*, Memorandum to Distribution, Sandia National Laboratories, Albuquerque, New Mexico.

1. PURPOSE

This report documents the post-closure disposal criticality evaluation of a generic waste form without moderation control at the Waste Isolation Pilot Plant (WIPP) using criticality control overpacks (CCOs) and is very similar to a previous report that analyzed a more specific plutonium disposition waste form [1]. This activity supports the viability assessment for geologic disposal of plutonium. Results of this evaluation and others like it will be used to support the Sandia National Laboratory (SNL) future impact assessments of the WIPP repository.

The scope of this assessment is focused on long-term waste disposition in CCOs through the repository's performance period of up to 10,000 years. CCOs are designed to contain fissile gram loadings of up to 380 fissile gram equivalent (FGE) ^{239}Pu, which is higher than other waste containers' loadings currently approved for disposal at WIPP. The scenarios analyzed that can impact criticality potential include (1) initial room closure/collapse from initial emplacement, hereafter referred to as the *reconfigured dry* scenario (*dry* does not necessarily mean a fast neutron spectrum as there is moderating material within the waste form that can affect the neutron spectrum), and (2) flooding with brine, hereafter referred to as the *reconfigured wet* scenario. Drying out of the reconfigured wet scenario is also considered. External repository scenarios resulting from potential movement and reconfiguration after a brine intrusion event are also discussed.

The software used to perform the calculations in this report is described in Section 2. Direct inputs that were used in the development of this technical product and for making final conclusions are documented in Section 3. Section 4 describes the assumptions used in the absence of direct confirming data or evidence to perform the modeling and analyses documented in this report. A description of the different analyses performed and the systems, processes, and phenomena considered to assess criticality potential over the WIPP post-closure period are provided in Section 5. Conclusions of this report are documented in Section 6. The appendices are as follows: Appendix A provides information on calculating input specifications for the neutronics analyses; Appendix B documents calculational results; Appendix C provides a listing of how the input and output files for this report are organized; and Appendix D documents the computational model validation.

2. SOFTWARE AND CALCULATIONS

The calculations for this investigation were performed using the SCALE code system [2], version 6.2.3. The Criticality Safety Analysis Sequence (CSAS) with KENO V.a (CSAS5) was used to calculate neutron multiplications factors (k-effective [k_{eff}] values). All cases were performed with ENDF/B-VII.1 cross section data in the 252-group library using CENTRM to provide problem-dependent multigroup cross section processing on the Romulus computer cluster. Romulus is maintained under the configuration control of ORNL's Reactor and Nuclear Systems Division (RNSD) staff.

All calculations were run with sufficient numbers of neutron histories (generations, neutrons per generation, and generations skipped) to yield converged results that passed the appropriate statistical checks. Plots of k_{eff} by generation and k_{eff} by generation skipped found in the output files showed that the k_{eff} eigenvalue was essentially flat for all active generations for all cases. Fission source convergence was verified by the Shannon entropy tests. The results are reported as k_{eff} plus two times the standard deviation (k-effective + 2 sigma, or $k_{eff} + 2\sigma$).

As with any computer code/calculation used for safety analyses and assessments, the ability of the calculation methodology to prove a configuration subcritical is obtained through a validation process. Appendix D contains the calculational validation for this report.

All input and output files are available on request as electronic media.

3. DATA USED TO DEVELOP MODELS

The WIPP underground disposal repository consists of multiple salt panels mined from the Salado formation, a 2,000 ft–thick series of salt beds. A typical underground panel includes several rooms, each of which is approximately 33 ft wide by 13 ft high by 300 ft long. Magnesium oxide (MgO) is used as backfill; bags of MgO are placed on top of and possibly around the container stacks.

The main focus of this report is on the CCOs, but additional waste containers are allowed at the WIPP. Transuranic (TRU) waste is currently authorized to be shipped to the WIPP from DOE generator sites in a limited number of approved shipping containers. The approved contact-handled (CH) Type B shipping packages (for materials with high levels of radioactivity) include the TRU Package Transporter Model II (TRUPACT-II), the Half-Package Transporter (HalfPACT), and the TRUPACT-III. Waste containers shipped in TRUPACT-IIs and HalfPACTs include 55, 85, and 100 gal drums; shielded containers; standard waste boxes; ten-drum overpacks; CCOs; and pipe configurations overpacked in 55 gal drums. The standard large box is shipped in the TRUPACT-III. Documents containing the transportation analyses include container descriptions and nuclear criticality safety evaluations for these various containers. These documents include the following:

- *TRUPACT-II Safety Analysis Report* [3],
- *Contact-Handled Transuranic Waste Authorized Methods for Payload Control (CH-TRAMPAC)* [4], and
- *CH-TRU Payload Appendices* [5].

The following sections discuss the information used to develop the calculational models.

3.1 WASTE CONTAINERS

3.1.1 CCO

The CCO consists of a criticality control container (CCC) within a standard 55 gal drum held in place by laminated plywood dunnage assemblies (Figure 1). *Criticality Control Overpack* [6] is a drawing of the container and *Specification for Fabrication of the Criticality Control Overpack* [7] is the container's specification document. The CCC is a stainless-steel schedule 40 cylindrical pipe (nominal pipe size/diameter of 6 in. [NPS 6]) constructed of 304 stainless steel with a blind flange welded bottom cap and a blind flange bolted to a slip-on flange, with a gasket providing a sealed lid.

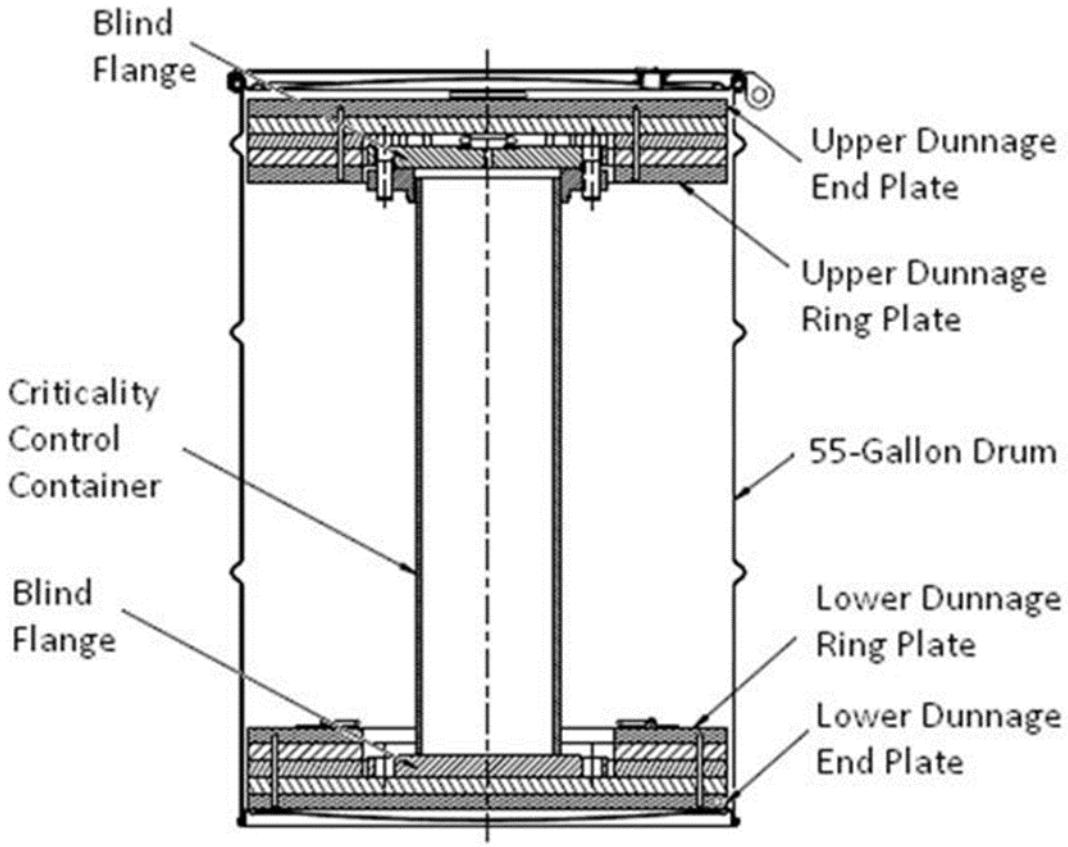

Figure 1. Criticality control overpack.

CCOs are typically handled in seven-pack arrangements for transport and storage. This is similar to the method used for handling 55 gal drums. The seven-packs of drums are stacked two high inside TRUPACT-II containers for transport and are stacked three high for disposal at WIPP.

Criticality safety analyses for the transport and initial emplacement of CCOs already exist. *Criticality Control Overpack Criticality Analysis for TRUPACT-II and HalfPACT*, 01937.01.M009-1 [8], is the criticality safety analysis for transport of CCOs, and *Nuclear Criticality Safety Evaluation for Contact-Handled Transuranic Waste Containers at the Waste Isolation Pilot Plant*, WIPP-016 [9], is the criticality safety analysis for initial emplacement and storage of CCOs at WIPP.

A base calculational model was developed from the CCC/CCO drawings [6] and specifications [7] in Reference [1]. Table 1 lists the dimensions. The CCC/CCO dimensions were relied on only as a starting point before the room closes in and the geometry begins to change.

Table 1. CCC/CCO characteristics.

	Inches	Centimeters	Notes
CCO characteristics			
Outer diameter	22.618	57.45	Inner diameter plus wall thickness from CQ5508A5[a] (0.15 cm/0.0590 in. [16 gauge])
Outer radius	11.309	28.725	
Inner diameter	22.50	57.15	From CCO-DWG-0001R3
Inner radius	11.25	28.575	
Wall/top/bottom thickness	0.059	0.15	From CQ5508A5, 16 gauge (drawing gives range of 0.0543 to 0.0590 in.)
Outside height (including bolt ring)	34.75[b]	88.265	Outside height of drum from CQ5508A5[a] (34.25 in.) + 0.5 in. (conservative underestimate of height added from bolt ring)
Outside height (drum only, not including additional height from bolt ring)	34.25	86.995	From CQ5508A5, includes additional height from curvature of top and bottom of drum (underestimate of 0.691 in. for each) and top and bottom thickness
Inner height (at outermost edge)	32.75	83.185	From CCO-DWG-0001R3 (does not include drum top and bottom thickness)
Material			Carbon steel
CCC characteristics			
Outer diameter	6.625	16.8275	From CCO-DWG-0001R3, nominal pipe size (NPS) 6, SCH 40
Outer radius	3.3125	8.4138	
Wall thickness	0.28	0.7112	
Inner diameter	6.065	15.4051	Outer dimension minus wall thickness
Inner radius	3.0325	7.7026	
Flange thickness	1.0	2.54	From CCO-DWG-0001R3, CLASS 150, NPS 6, top and bottom (diameter/radius may be modeled same as CCC pipe outer dimension)
Flange diameter	11.02	27.9908	
Flange radius	5.51	13.9954	
Ring gasket	1/16	0.1588	From CCO-DWG-0001R3, NPS 6, 1/16 THK
Cavity height	26.9425	68.4340	From CCO-DWG-0001R3 (26.50 + 0.38 + (1/16 in.), includes additional space from gasket
Material			From CCO-DWG-0001R3, stainless steel 304, use code standard composition
Dunnage characteristics			
Thickness	3/4	1.905	From CCO-DWG-0001R3, all plates (total of 10 plates— 2 end and 3 ring plates on bottom and 2 end and 3 ring plates on top
Outer diameter	22.0	55.88	
Outer radius	11.0	27.94	
Ring plate inner diameter	11.5	29.21	From CCO-DWG-0001R3
Ring plate inner radius	5.75	14.605	
Material			Plywood with density of 0.387 g/cm^3 (SCALE redwood standard composition)

[a] = CQ5508A5 is the drawing for the 55 gal drum, as referenced in CCO-DWG-0001R3.
[b] = The total drum height (34.75 in.) includes the spacing created by the curvature of the top and bottom of the drum and the spacing created by the bolt ring.

The total drum height (34.75 in., listed as outside height in Table 1) is modeled as follows:

bottom thickness	+	curvature space	+	inner height at outermost edge	+	curvature space	+	top/lid thickness	+	bolt ring space
0.059	+	0.691	+	32.75	+	0.691	+	0.059	+	0.5

The inner drum height (32.75 in.) is modeled as follows:

bottom end plate dunnage	+	bottom flange	+	cavity height	+	top flange	+	hoist ring space	+	top end plate dunnage	+	handle space
1.5	+	1.0	+	26.9425	+	1.0	+	0.5	+	1.5	+	0.3075

Figure 2 shows an approximation of the total drum height and the inner drum height in relation to Figure 1. The handle located above the top end plate dunnage requires approximately 0.5 in. of vertical space. Even though this handle space puts the inner drum's height at greater than 32.75 in., it does not create an issue because the handle is at the center; the actual space available includes the spacing created by the upper curvature of the drum lid.

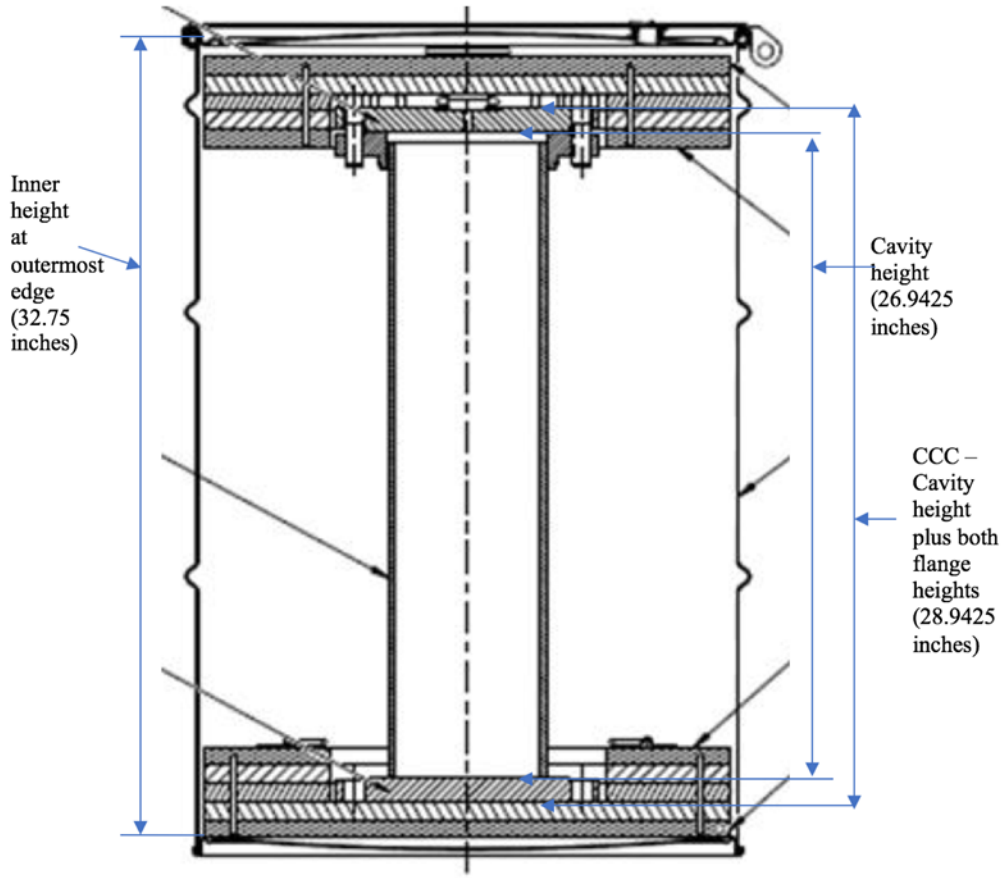

Figure 2. Criticality control overpack total and inner drum height specifics.

3.2 WASTE FORM

The fissile material present in the waste form was quantified in terms of ^{239}Pu FGE and was specified in the calculational models as ^{239}Pu. This is consistent with fissile material loadings specified in the *TRUPACT-II Safety Analysis Report* [3] and in the specifications and calculations in its associated documents and container analyses. ^{239}Pu was used to bound all fissile isotopes that could be present. For compliance purposes, fissile isotopes other than ^{239}Pu were converted to ^{239}Pu FGE using fissile gram equivalents that can be found in the *Contact-Handled Transuranic Waste Authorized Methods for Payload Control*, *CH-TRAMPAC* [4]. This is also considered bounding of decay and isotopic changes to the fissile material that would occur over the disposal period.

The waste form model in this analysis is more generic than the plutonium disposition waste form in Reference [1] and is more similar to the generic waste form in Reference [8] and Reference [9] as well as the other models used for analyses supporting the TRUPACT-II safety analysis [3]. All of the generic waste models supporting the TRUPACT-II safety analysis are a mixture of water and polyethylene with beryllium added to bound any special moderators that might be present. The water/polyethylene mixture is considered bounding of all types of waste; therefore, there are no restrictions or requirements on the specific makeup of the waste form outside of the fissile material, beryllium, and B_4C content. The waste form modeled in this analysis is a mixture of 75% water and 25% polyethylene (modeled as CH_2). Variations of 100% water and 100% polyethylene were also considered for comparison. The amount of fissile material per container is 380 FGE ^{239}Pu, modeled as PuO_2, mixed homogeneously with the other materials. The total amount of the water/polyethylene mixture per container is varied to determine the optimum moderation to fissile material (H/Pu) ratio. See Appendix A for discussions on how the material mixture make-up was determined.

The waste form in this analysis uses a base mixture of 75% water and 25% polyethylene, the total amount of which is varied to determine the optimum moderation to fissile material (H/Pu) ratio.

For closure scenarios, a neutron absorber is added to the models in order to ensure subcriticality. The neutron absorber is modeled as different amounts of B_4C in support of process optimization considerations, with the boron content considered as natural boron (19.9 wt% ^{10}B, 80.1 wt% ^{11}B).

Other waste containers typically allow beryllium to be included for up to 1% by weight of the waste content [3, 4, 5] and may also be present in oxide form. As listed in Reference [4], the empty weight for a CCO was 104.3 kg (230 lb), with a maximum gross weight of 158.8 kg (350 lb), which resulted in a maximum waste weight of 54.5 kg. The beryllium content (1% by weight) is based on the total allowed waste weight (does not include packaging and container weights). Therefore, the 1%-by-weight limit for beryllium was determined to be 545 g, which is consistent with other container limits. Cases were run with 545 g of beryllium per CCO intermixed in the waste form.

The waste form used for this criticality assessment can be described as follows:

- maximum of 380 FGE ^{239}Pu per CCO;
- maximum beryllium content of 545 g per CCO;
- no restriction on the amount of water or polyethylene present in the CCO;
- minimum credited B_4C content, intermixed within the waste form, of 50 g per CCO; and

- no restrictions or requirements on the specific makeup of the waste form outside of the fissile material, beryllium, and B_4C content.

3.3 BRINE INTRUSION

The most significant potential for brine intrusion results from human intrusion events that would involve borehole drilling into the disposal area and a postulated underlying source of pressurized brine. See Section 5.3 for more details. Therefore, brine intrusion (flooding) scenarios modeled the intruding fluid as a saturated brine (water with salt). The saturated brine composition was modeled based on the geochemistry of the area [10], with a molality of 5.98 mol of salt/kg of H_2O. See Appendix A for the number densities.

4. ASSUMPTIONS

4.1 SCENARIOS TO BE CONSIDERED/MODELED

Assumption: Scenarios considered/modeled were post-closure scenarios involving changes to static storage after initial emplacement.

Basis: Utilizing same assumptions/justifications as in Reference [1].

4.2 CCC GEOMETRY AFTER ROOM CLOSURE

Assumption: The CCC geometry was assumed to remain in a cylindrical configuration for the reconfigured dry room closure scenarios.

Basis: Utilizing same assumptions/justifications as in Reference [1].

5. ANALYSIS DISCUSSION

This report documents a supplemental analysis to Reference [1] to document the ability of the 50 g B_4C to maintain a system k_{eff} of less than 1.0 during post-closure conditions with no restrictions on the amount of water or polyethylene. This report investigates scenarios associated with long-term storage of the generic water/polyethylene waste form in CCOs at WIPP over a 10,000 year performance period following closure (after transport and initial emplacement). The configurations used to determine the system k_{eff} for various amounts of moderation are provided in the subsequent sections.

5.1 CONFIGURATIONS MODELED

This investigation focuses on configurations after repository closure (same as Reference [1]), when the salt will creep/collapse around the containers [11]. The combination of room collapse and drum collapse results in an infinite number of possible changes to the geometric arrangement. Similar to what was done in Reference [1], this report analyzes uniform closure scenarios for two different configurations—infinite array and triangular-pitched array room models—to assess the impact of room closure effects on system k_{eff}.

Two scenarios were evaluated in Reference [1]: post-closure scenarios of room closure from salt creep (referred to as the *reconfigured dry scenario*), and flooding with brine [11] (referred to as the *reconfigured wet scenario*). Even though brine is expected to reduce the system k_{eff}, as shown in References [1] and [12], it is included in this report since it leads to further container degradation and array compaction which are expected to increase the system k_{eff}. To support these investigations, some modeling simplifications were implemented that result in a net increase in the system k_{eff} and are thus conservative for the intended application. They are the same simplifications used in Reference [1] and are summarized below.

Models are either an infinite array of CCOs or a defined room model (disposal room) filled with CCOs. Common modeling attributes of the different configuration categories are as follows:

- Salt (halite) floors and ceilings were included, with a nominal thickness of 10 ft at a density of 135.2 lb/ft^3 (2.165 g/cm^3); when included, walls were modeled in the same manner.

- A 25 in.–thick continuous layer of MgO was modeled above the top layer of drums, between the drums and the salt ceiling, at a density of 90.5 lb/ft^3 (1.45 g/cm^3), to account for the MgO supersacks. This is consistent with the models used in the analysis for initial emplacement [8] and in Reference [1].

- Due to the exclusion of the carbon steel in the CCO drum and the plywood dunnage, the calculations documented in this report are simplified to model the waste containers as having the CCC height only. The actual initial CCO height (drum height) would also include voids created by the container structure (e.g., the bolt ring, lift attachments, curvature of the container top and bottom, as described and shown in Section 3). Substantial structure to maintain these spaces long term would be limited by the use of thin carbon steel. The omission of the plywood dunnage and the carbon steel CCO drum resulted in the drum height being modeled as the CCC height (28.9425 in. [73.514 cm]).

- The 304 stainless steel of the CCC was modeled.

- The full flange diameter was not modeled. Instead, the flange was modeled with the diameter of the CCC. Since the flange diameter is larger than the pipe diameter, the presence of the full flange

diameter would result in increased spacing between fissile material units and more material to interfere with neutron interaction, so omitting it is considered conservative for criticality analyses.

- The water/polyethylene waste form with 380 FGE ^{239}Pu was modeled in all CCCs.
- The waste form was centered axially in each CCC.
- CCCs were modeled as being stacked three high.
- No credit (i.e., negative reactivity benefit) was taken (modeled) for any inner, smaller metal containers.

Reference [1] showed two different configurations with the above simplifications—an infinite-array model and a triangular-pitched-array room model—as bounding of the scenarios analyzed. Brief descriptions of each model follow.

Infinite Array Model. Because the size of the disposal room is so large—approximately 33 ft wide by 300 ft long by 13 ft high—this configuration represents the room as a triangular-pitched array infinite in the *x* and *y* directions. An infinite array was simulated by placing mirror reflection boundaries on the sides (*x* and *y* directions) of the base unit. Figure 3 and Figure 4 show the top and side views, respectively, of the array base unit.

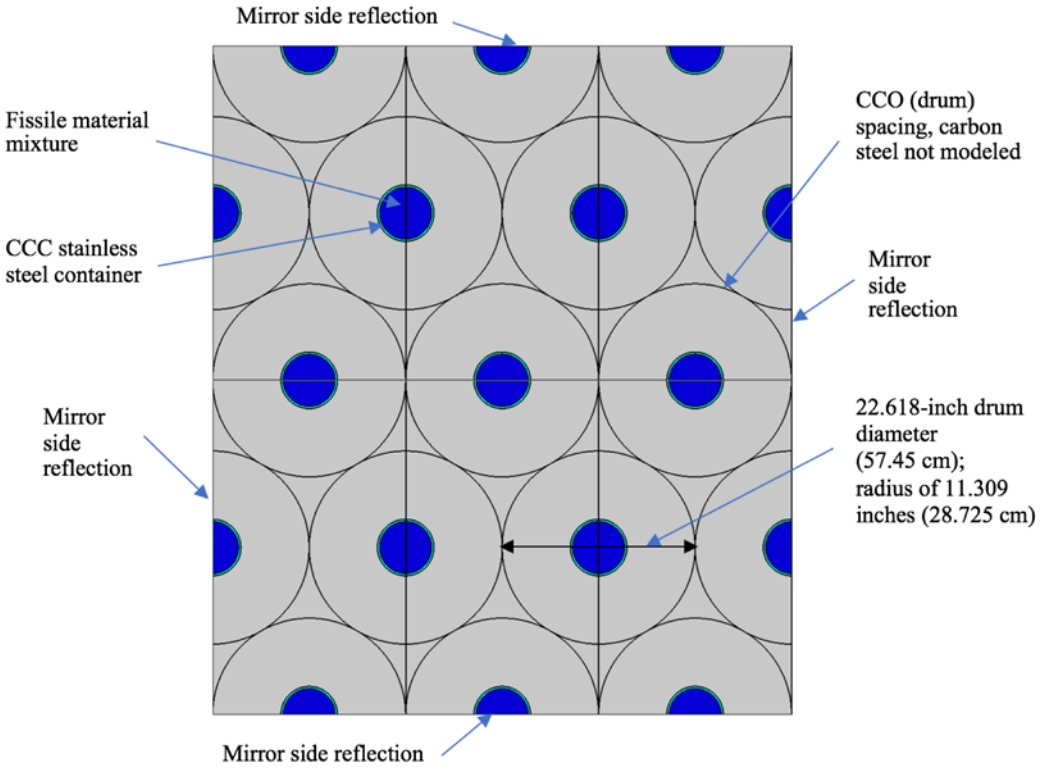

Figure 3. Top view of the base unit.

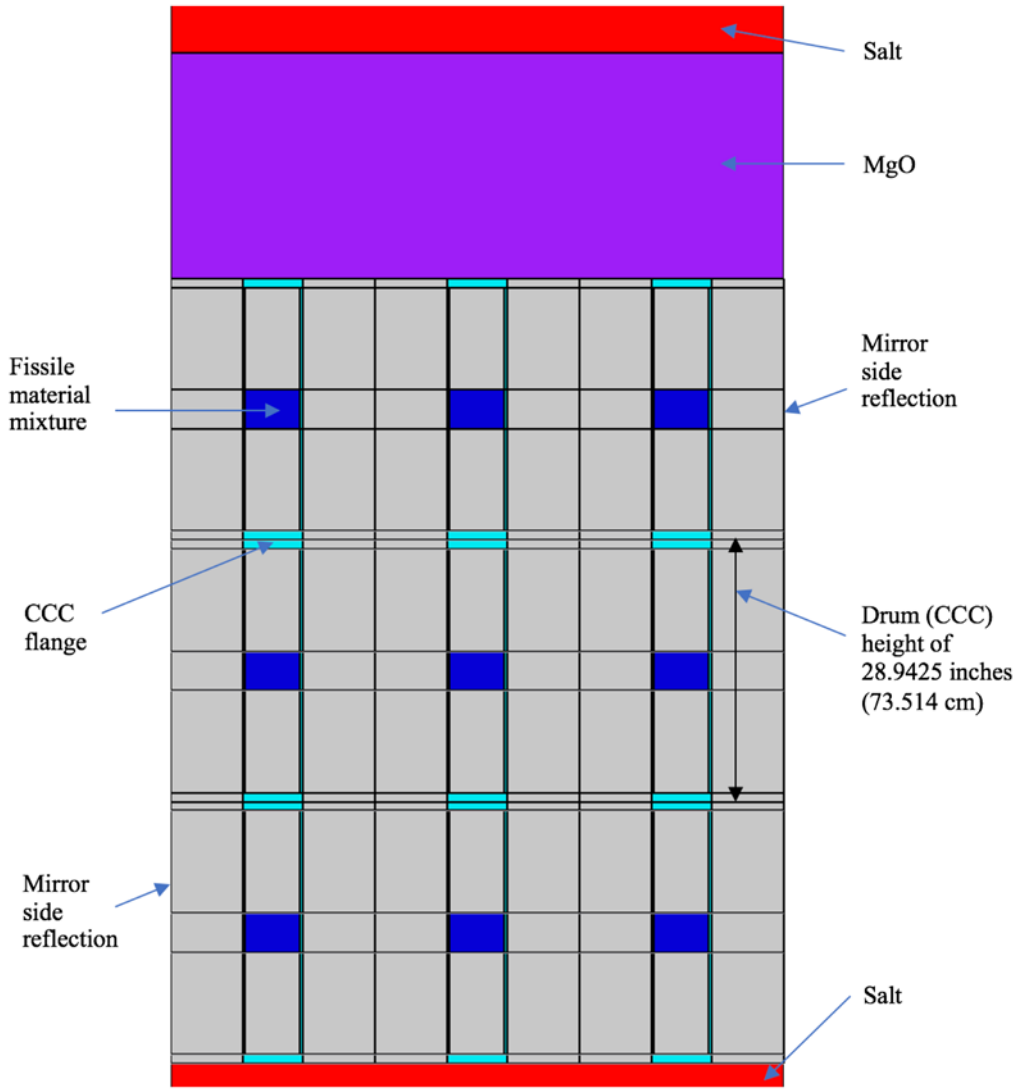

Figure 4. Side view of the base unit.

As shown in Figure 4, the fissile material waste form (or item) was modeled in the center of each CCC. This modeling arrangement is consistent with the existing analyses for handling and initial storage at the WIPP [9]. No credit (i.e., negative reactivity) was taken for the fissile material mixture container; no inner container(s) (inside the CCC) was/were modeled. The fissile material waste form was modeled as a cylinder with a diameter equal to the inner diameter of the CCC: 6.065 in. (15.4052 cm). This model does not account for neutron leakage in the *x* or *y* directions that would be caused by walls around a finite array (finite room model).

The modeled room height of ~9.3 ft was three times the modeled drum height (~7.2 ft [220.6 cm]) plus the MgO height (~ 2.1 ft [63.5 cm]) and was the same for all configurations.

Triangular-Pitched Array Room Model. This model takes the infinite array model and adds walls to account for side neutron leakage. The size of the modeled room is based on the initial room dimensions as described in Reference [1]. Figure 5 shows a partial top view of this configuration.

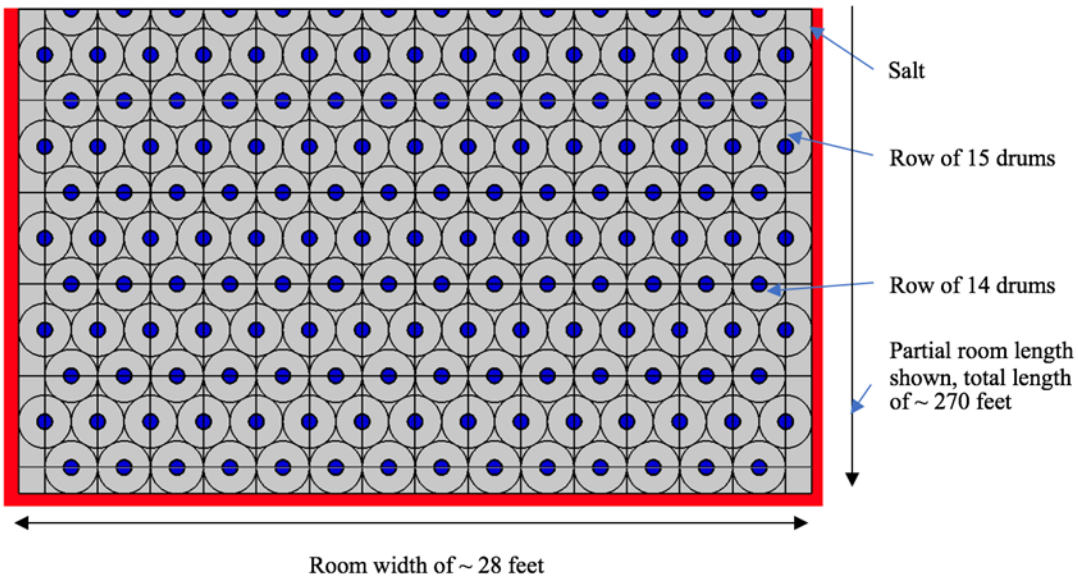

Figure 5. Partial top view of triangular-pitched array in room.

The drums are arranged in alternating rows of 14 and 15 drums across. The room was modeled with a width of ~28 ft and includes 83 rows of drums 14 across, alternating with 82 rows of drums 15 across, which totals to 7,176 drums and gives a room length of ~270 ft.

Both the infinite-array and the triangular-pitched (room) array were modeled with the water/polyethylene waste model. The amount of the water/polyethylene mixture modeled per CCC was varied to show how the system k_{eff} changed as the H/Pu ratio was varied. Figure 6 shows the results.

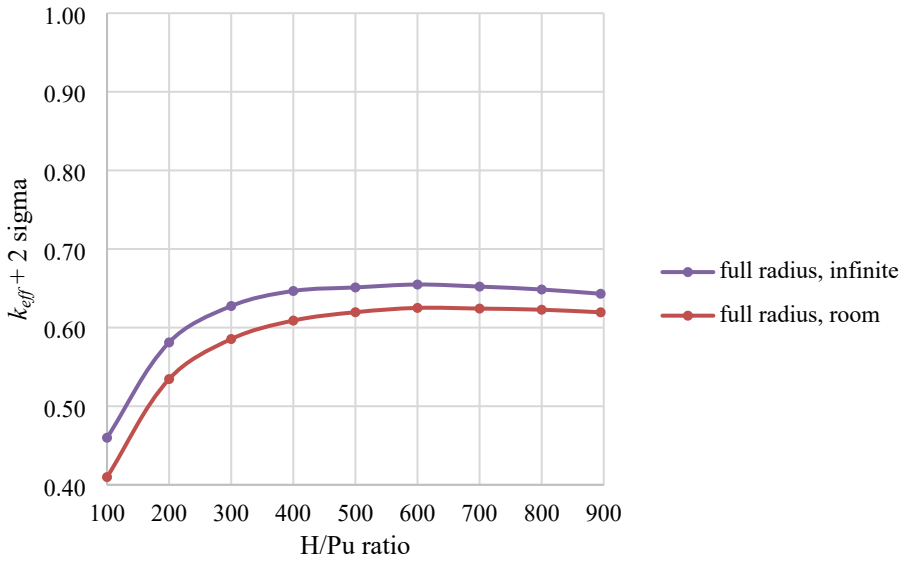

Figure 6. System k_{eff} as a function of the H/Pu ratio with 50 g of B_4C per CCO.

As shown in Figure 6, the more realistic room configuration has a lower system k_{eff}, through out the range of H/Pu ratios.

5.2 RECONFIGURED DRY SCENARIOS

5.2.1 CCOs

Reference [1] showed that the system k_{eff} increases with decreases in the *x* and *y* direction spacing and then increases further with decreases in the *z* direction spacing. The dry scenarios modeled here show the same trend.

Evaluations were performed by starting with a geometric arrangement representative of the as-emplaced configuration and then incorporating the effects caused by salt pushing the containers together, compressing or compacting the model by decreasing the spacing between fissile materials. These cases assumed that the CCC remains intact (see Assumption 4.2) with the spacing changes in the radial direction. The infinite array easily bounds this scenario, but it does not account for neutron leakage at the room's walls. Hence it is considered overly conservative. The full room triangular-pitched array takes credit for the room leakage, so the three-high triangular-pitched array with CCC pitch at 16.8 cm, in which CCCs are touching in vertical and radial directions, is identified as the limiting dry design basis configuration for simulating a disposal room full of CCOs. Figure 7 shows top and side views of this configuration. Due to dry conditions, no mechanism has been identified to degrade the CCC such that the vertical spacing would decrease in these dry scenarios. These cases are recognized as being very conservative since they do no credit any geomechanical models that demonstrate nonuniform closure with some spacing between CCOs. That analysis will be covered in other evaluations.

Radial compaction was modeled in steps: full radius (as shown in Figure 4 and Figure 5), radius decreased by 7 cm, radius decreased by 14 cm, and radius decreased by 20 cm (full compaction with CCCs touching, as shown in Figure 7). The amount of B_4C added to the waste mixture was varied from zero to 200 g per CCC. The results are shown in Figure 8. These cases all use the room model with an H/Pu of 200.

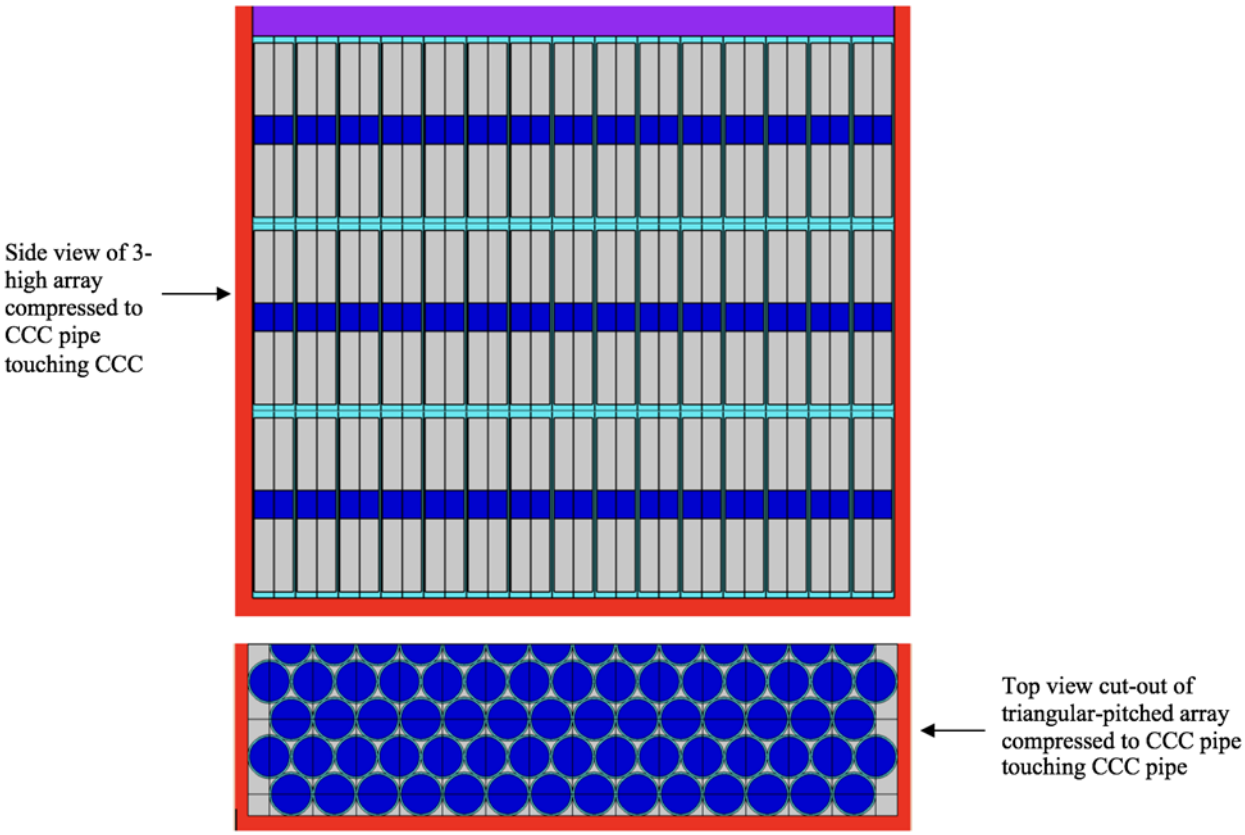

Figure 7. Top and side views of full radial compaction configuration.

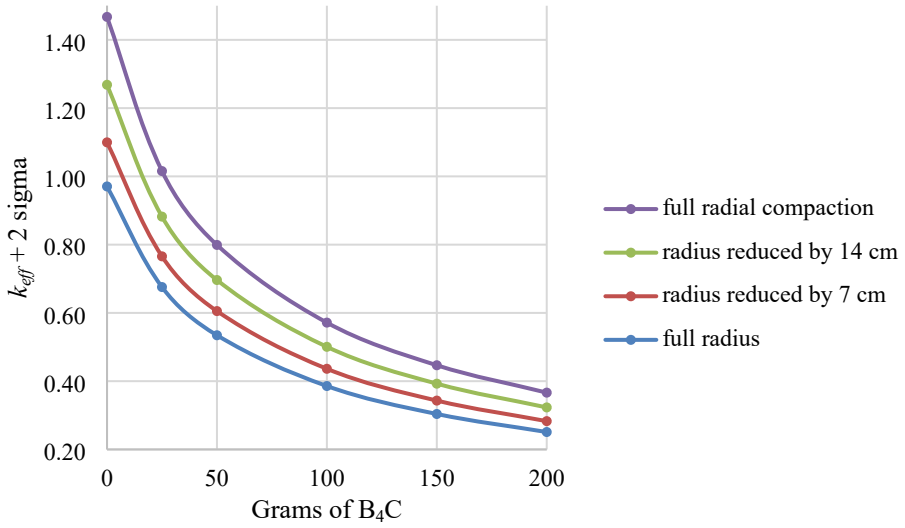

Figure 8. Results for incorporating B_4C into the fissile material mixture (H/Pu of 200).

The cases presented in Figure 8 show that, with 50 g of B_4C mixed with the waste form, the k_{eff} for all spacing configurations is less than 1.0.

For comparison, the full radial compaction room array model was analyzed at different H/Pu ratios with different amounts of B_4C, ranging for 25 to 200 g. Figure 9 shows how the results are clustered; the optimum H/Pu ratio is approximately 300 (no vertical compaction).

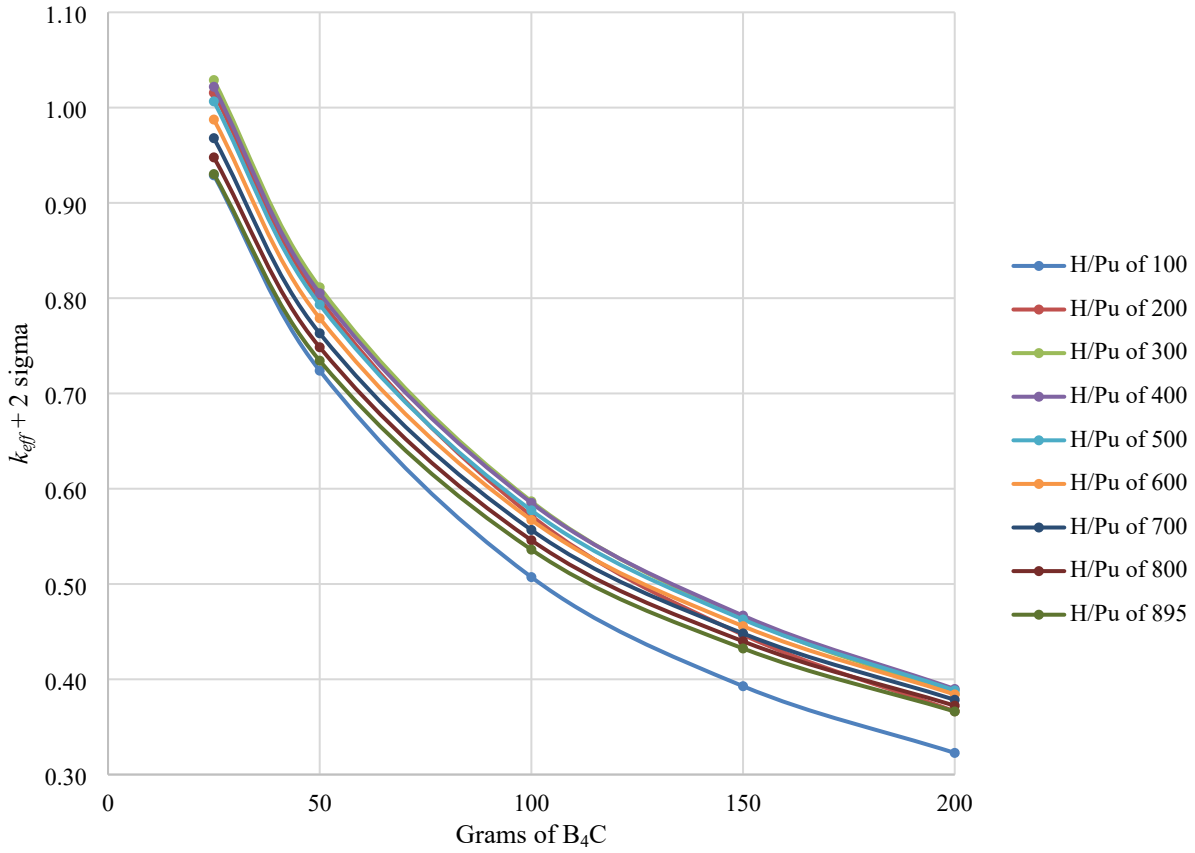

Figure 9. Results for different amounts B_4C with different H/Pu ratios.

5.3 RECONFIGURED WET SCENARIOS

Brine entry due to dewatering of the surrounding Salado halite allows brine to enter the disposal area. However, the most significant source of brine is from a human intrusion event that must be considered during long-term disposal. According to the 2014 Compliance Recertification Application [13], DOE identifies multiple scenarios for consideration. The scenarios that could lead to flooding in the disposal rooms are deep drilling scenarios. A deep drilling scenario would involve creation of one or more boreholes intersecting the disposal room, with at least one of these boreholes also penetrating a postulated underlying source of pressurized brine, so any resultant flooding would not involve "pure water," but would instead involve a saturated brine that may have other elements present in addition to salt.

Similar to Reference [1], the equilibrated brine composition as defined in Reference [10] and modeled here has a molality of 5.98 mol (moles per kilogram of H_2O). Three different brine intrusion scenarios were examined: (1) brine intrusion with the CCCs intact, (2) brine intrusion with the CCCs degraded, and (3) migration of disposal area materials to external areas after brine intrusion.

5.3.1 Brine Intrusion with CCCs Intact

The first brine intrusion scenario involves modeling the void spaces in and/or around the CCCs as filled with saturated brine (equilibrated brine as defined in Reference [10]). Both the infinite array and room array models are analyzed in two scenarios (1) with brine outside the CCCs and (2) with brine also inside the CCCs and filling all voids. All models have full radial compaction. Figure 10 shows the results.

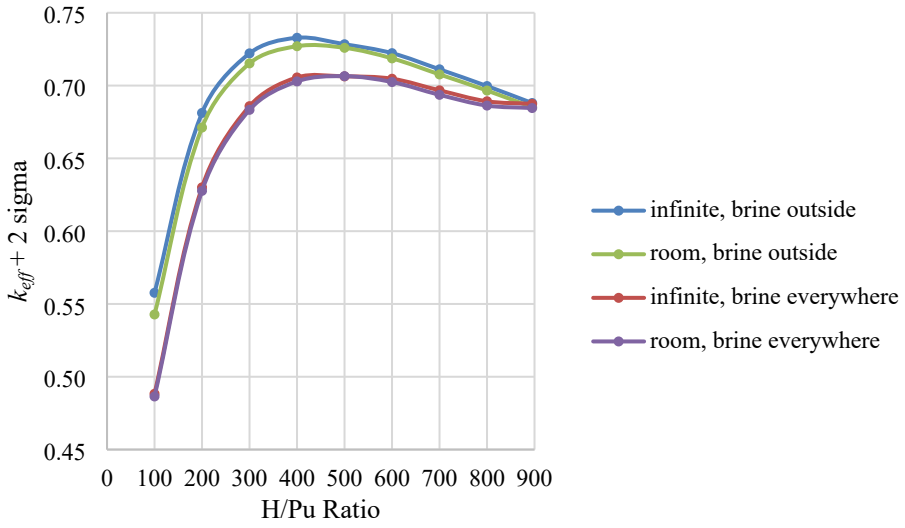

Figure 10. Results for flooding with brine.

Brine intrusion scenarios are presented in Reference [1], with the CCOs in the Triangular-Pitched Array Room Model. Similar to the results in Reference [1], these cases show that all configurations with equilibrated brine result in lower system k_{eff}s when compared with the cases involving dry configurations with the CCCs intact. The optimum moderation level has shifted to a slightly higher H/Pu ratio compared to the dry configurations.

5.3.2 Brine Intrusion with CCCs Degraded

After the brine enters the repository, the waste container materials are expected to undergo corrosion and degradation. As the scenario progresses, a mixture of brine and corrosion products would surround the fissile material items in the room. This mixture is expected to continue to change over time as the waste container packaging corrodes and dissolves into the brine mixture. An infinite number of potential configurations could be modeled considering the different rates of reaction, resulting precipitation products, and the way these materials will change over the post-closure period. In this scenario, the corrosion of the packaging leads to vertical compaction with the potential degradation of the CCCs. To bound this and the drying-out period that may follow, the infinite-array and room-array configurations are modeled with full vertical compaction (no voids inside the CCCs) along with full radial compaction, as shown in Figure 11.

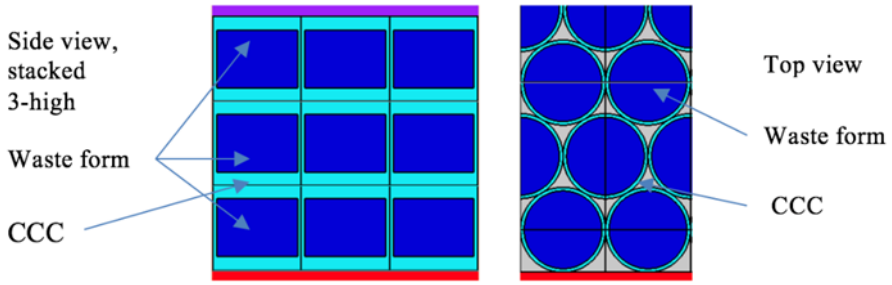

Figure 11. Top and side views of full vertical compaction along with full radial compaction.

The configurations are modeled with and without brine, with results shown in Figure 12.

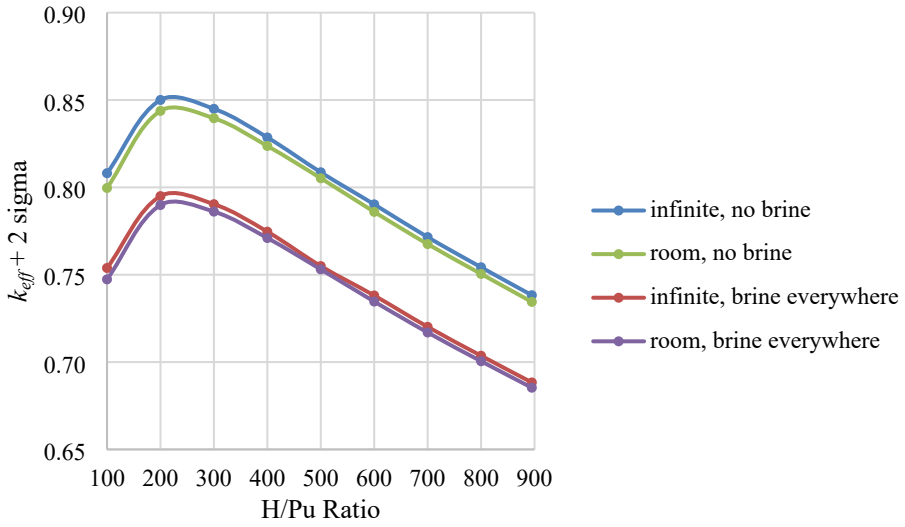

Figure 12. Results for full vertical and radial compaction, with and without brine.

These results have slightly higher system k-effectives, as expected with the vertical compaction. The optimum moderation is also at a slightly different H/Pu ratio.

Configurations of the 3-tier room array collapsing to a 2-tier room array were also analyzed. Two scenarios were modeled. In the first scenario, the 3rd tier combines with the 2nd tier. In the second scenario, the 3rd tier combines with the 1st and 2nd tier so that each tier has an equal number of CCOs. All of the cases modeled the CCOs with full vertical compaction, with an H/X of 200, with 50 g of B_4C per CCO, and with no brine present. For each scenario/configuration, the same number of rows are modeled; the combined CCOs are added to the width of each array.

For the first combined tier scenario of the 3rd tier combining with the 2nd tier, three configurations were modeled. For all three configurations the combined tier CCOs are modeled with full radial compaction. The bottom tier CCOs are modeled with first no radial compaction, second with enough compaction to approximate the width of the combined tier, and third with full radial compaction.

For the second combined tier scenario of the 3rd tier CCOs equally split between the 1st and 2nd tiers, two configurations were modeled. In the first configuration, the CCOs had enough radial compaction so that the width of the compacted array was approximately the same as the original room width. In the second configuration all CCOs are modeled with full radial compaction.

The results are listed in Table X and show the 3-tier array to be bounding of the 2-tier array configurations. The 3-tier array with full radial and vertical spacing and with full radial and vertical compaction are included for reference.

Table 2. Comparison of scenarios with USLs.

Case Description	k_{eff}	sigma	$k_{eff} + 2\sigma$
For reference			
Room array (3 tier), H/Pu of 200, 50 g B_4C per CCO, full radius (no compaction)	0.5343	0.0001	0.5345
Room array (3 tier), H/Pu of 200, 50 g B_4C per CCO, full radial and vertical compaction	0.8436	0.0001	**0.8438**
3rd tier combined with 2nd tier			
Room array, H/Pu of 200, 50 g B_4C per CCO, bottom tier with no radial compaction	0.7733	0.0001	0.7735
Room array, H/Pu of 200, 50 g B_4C per CCO, bottom tier radially compacted to combined tier width	0.7843	0.0001	0.7845
Room array, H/Pu of 200, 50 g B_4C per CCO, bottom tier with full radial compaction	0.8229	0.0001	0.8231
3rd tier split between 2nd and 1st tier			
Room array, H/Pu of 200, 50 g B_4C per CCO, radially compacted to original room width	0.6544	0.0001	0.6546
Room array, H/Pu of 200, 50 g B_4C per CCO, full radial compaction	0.8259	0.0001	0.8261

For additional comparison, the no brine room model cases (full radial and vertical compaction), were run with the waste mix composition varied. The 75% water, 25% polyethylene was replaced with 100% water, 100% polyethylene, and 100% polyethylene at twice the theoretical density. Figure 13 shows the results. Neither the 100% water or 100% polyethylene cases vary significantly from the 75%–25% mix, with the polyethylene density doubled, the peak k_{eff} is only increased by about 0.01.

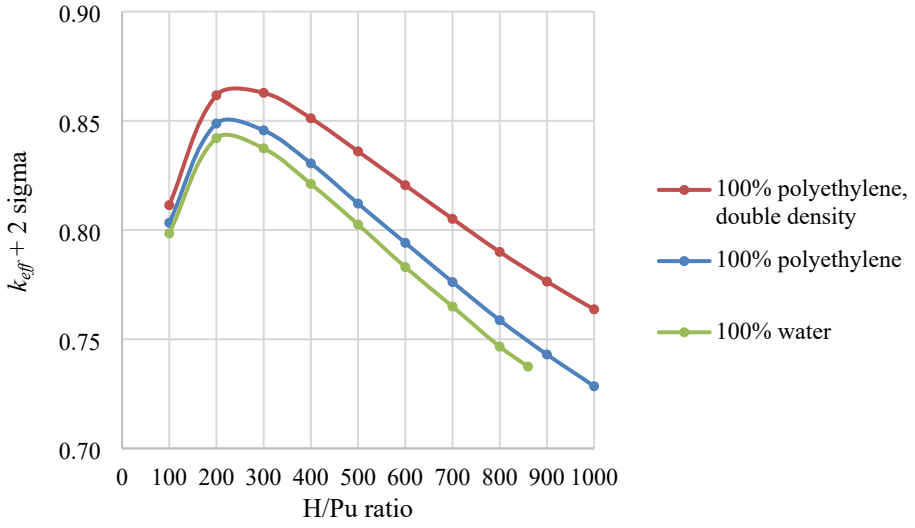

Figure 13. Results for varying the waste mix water/polyethylene content.

The MgO sacks are expected to rupture over time; however, the above degradation cases do not consider the MgO sacks rupturing and spilling their contents between the CCOs. The exact amount of MgO that could end up between the CCOs is difficult to determine. It is not expected that there will be enough MgO to completely fill the space, but an accumulation is expected. To bound the scenario, cases (with the room configuration) were modeled with MgO completely filling the space in three arrangements: no compaction, full radial compaction, and full radial and vertical compaction. Figure 14 shows the results. The added MgO reflection does not have a significant effect on the system k_{eff}.

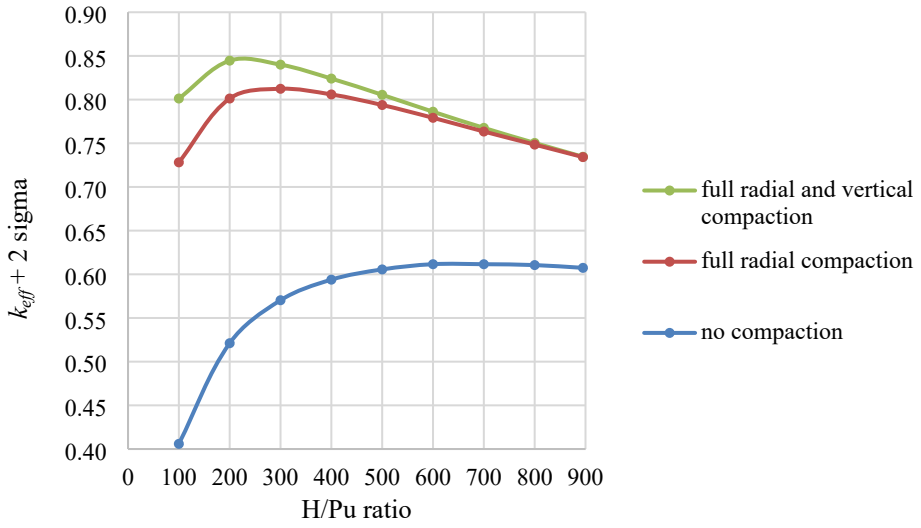

Figure 14. Results with MgO between the CCOs.

5.3.3 Migration of Materials after Brine Intrusion to External Areas

Once a room is flooded, the potential for material migration to other areas outside the disposal room must also be considered. Previous analyses [14, 15] have shown that criticality external to the repository is not credible due to three arguments: (1) the amount of fissile material transported over 10,000 years is predicted to be small, (2) there are insufficient spaces to provide sufficient thickness for precipitation of fissile material, and (3) there is no credible mechanism to counteract the natural tendency of the material to disperse during transport and instead concentrate fissile material in a small enough volume for it to form a critical concentration. All of those arguments are summarized in the performance assessment included in the Compliance Recertification Application [13].

The following information, stated in *Low Probability of Criticality Following Disposal of Surplus Plutonium at the Waste Isolation Pilot Plant* [16], is cited in considering the additional plutonium source inventory being addressed in this work: “Release of Pu at WIPP is solubility controlled; hence, an increase in the Pu inventory does not directly influence Pu release.” Therefore, the existing justification for external subcriticality is still applicable.

6. CONCLUSIONS

This report demonstrates that with the inclusion of B_4C, limits on moderator content (water and plastic content) are not necessary to demonstrate the subcriticality of fissile materials packaged using the CCO for disposal at WIPP. Criticality analysis results for multiple scenarios associated with post-closure of WIPP have been considered. Two scenario progressions were considered in this criticality assessment: *the reconfigured dry scenario* (i.e., room closure from salt creep) and the *reconfigured wet scenario* (i.e., flooding with brine). During the post-closure performance period at WIPP, the salt bed environment will slowly move over time to close and fill in fractures or holes between canisters. Vertical and horizontal closure may not occur at the same rate, and the forces exerted on the canisters will vary over time. Likewise, the rate of degradation of the waste containers or of their configuration is also not presumed to be known and will vary over the repository performance period. The waste configurations that could result from these closure scenarios are still being determined. Therefore, a conservative analysis approach was used.

Several configuration categories and waste form constituents were analyzed to assess the impact of the different types of changes that can occur after emplacement as a repository closure progresses. The objective was to evaluate a very conservative arrangement of waste container configurations with respect to impacts on criticality potential and to establish a limiting design basis configuration for the disposal criticality assessment. This report does not focus on the probability of any progression scenarios. Rather, it considers and bounds the most reactive credible scenarios that could occur.

The bounding configuration consists of a tight-packed triangular-pitched array of CCCs stacked three high. The analysis documented here supplements Reference [1] in demonstrating that for all scenarios, subcriticality is maintained when 50 g of B_4C (acting as a neutron absorber) per CCC is intermixed within the waste form, with no restrictions on the maximum moderation content (amount of water and/or polyethene or water- and/or polyethylene-like materials).

None of the configurations or results from this report challenges the chemistry and/or arguments supporting the existing analyses or their corresponding results. Therefore, the flooded scenario of fissile material migrating to an external area is bounded by existing analyses [14, 15, 16].

The calculational validation can be found in Appendix D. The validation results (bias and bias uncertainty) are used to develop upper subcritical limits (USLs). Calculated results below the USL are considered subcritical. Biases and bias uncertainties were determined by two different methods for comparison – by trending on correlation coefficients (c(k)s) determined by sensitivity/uncertainty methods and by trending on the energy of average neutron lethargy causing fission (EALF). See Appendix D for further details. Table 3 lists the results.

Table 3. Comparison of scenarios with USLs.

Scenario	Bias based on c(k)	Bias uncertainty	Bias for beryllium and chlorine	Administrative margin	USL
Dry reconfigured	0.0010	0.0294	0.0010	0.02	0.9486
Wet reconfigured	0.0005	0.0305	0.0014	0.02	0.9476
Scenario	**Bias based on EALF***	**Bias uncertainty**	**Bias for beryllium and chlorine**	**Administrative margin**	**USL**
All	0.0000	0.0159	NA	0.02	0.9641

*Positive bias set to 0

Based on the conservative USLs determined with c(k) trending, any dry scenario result ($k_{eff} + 2\sigma$) less than 0.9486 and any wet scenario result less than 0.9476 can be considered to be subcritical.

7. REFERENCES

[1] E. M. Saylor. 2017. *Nuclear Criticality Safety Assessment of Potential Disposition at the Waste Isolation Plant*, ORNL/TM-2017/751/R1, Oak Ridge National Laboratory, Oak Ridge, Tennessee.

[2] ORNL. 2018. *SCALE Code System*, ORNL/TM-2005/39, Version 6.2.3, Oak Ridge National Laboratory, Oak Ridge, Tennessee. Available from Radiation Safety Information Computational Center as CCC-834.

[3] DOE CBFO. 2013. *TRUPACT-II Safety Analysis Report*, Revision 23, US Department of Energy, Carlsbad Field Office, Carlsbad, New Mexico.

[4] DOE-CBFO. 2013. *Contact-Handled Transuranic Waste Authorized Methods for Payload Control (CH-TRAMPAC)*, Revision 4, US Department of Energy, Carlsbad Field Office, Carlsbad, New Mexico.

[5] DOE-CBFO. 2013. *CH-TRU Payload Appendices*, Revision 3, US Department of Energy, Carlsbad Field Office, Carlsbad, New Mexico.

[6] NWP. 2015. *Criticality Control Overpack*, CCO-DWG-001, Revision 3, Nuclear Waste Partnership, LLC.

[7] NWP. 2013. *Specification for Fabrication of the Criticality Control Overpack*, CCO-SPC-0001, Revision 2, Nuclear Waste Partnership, LLC.

[8] AREVA. 2012. *Criticality Control Overpack Criticality Analysis for TRUPACT-II and HalfPACT,* 01937.01.M009-1, Revision 0, AREVA Federal Services LLC.

[9] NWP. 2015. *Nuclear Criticality Safety Evaluation for Contact-Handled Transuranic Waste Containers at the Waste Isolation Pilot Plant,* WIPP-016, Revision 5, Nuclear Waste Partnership LLC.

[10] SNL. 2008. *Preparing Synthetic Brines for Geochemical Experiments*, Rev. 2, Activity/Project Specific Procedures, SP 20-4, Carlsbad, New Mexico: Sandia National Laboratories.

[11] DOE-CBFO. 2014. *Appendix SCR-2014 Feature, Event and Process Screening for PA*, DOE/WIPP-14-3503, US Department of Energy, Carlsbad Field Office, Carlsbad, New Mexico.

[12] B. Brickner. 2019. *Post Placement Nuclear Criticality Evaluations Involving 6- and 12-Inch Pipe Overpack TRU Waste Containers at the Waste Isolation Pilot Plant*, ORNL/TM-2019/1222/R0, Oak Ridge National Laboratory, Oak Ridge, Tennessee.

[13] DOE-CBFO. 2014. *Title 40 CFR Part 191 Subparts B and C Compliance Recertification Application 2014,* DOE/WIPP-14-3503, US Department of Energy, Carlsbad Field Office, Carlsbad, New Mexico.

[14] R. Rechard, L. Sanchez, C. Stockman, Holly T. 2000. *Consideration of Nuclear Criticality When Disposing of Transuranic Waste at the Waste Isolation Pilot Plant,* SAND99-2898, Sandia National Laboratories, Albuquerque, New Mexico.

[15] SNL. 1996. *RNT-1: Nuclear Criticality in Near Field and Far Field*, WIPP Compliance Certification Application (CCA) Reference 535, Sandia National Laboratories, Albuquerque, New Mexico.

[16] Rechard, R., Sanchez, L., Stein, E. and Xiong, Y. 2018. *Low Probability of Criticality Following Disposal of Surplus Plutonium at the Waste Isolation Pilot Plant*, Sandia National Laboratories, Carlsbad, New Mexico. ERMS 570596.

APPENDIX A. MATERIAL DESCRIPTIONS

A.1 GENERIC WASTE FORM

The waste form model is a generic waste form, similar to other generic waste models used for modeling waste. All of the generic waste models supporting the TRUPACT-II safety analysis are a mixture of water and polyethylene with beryllium added to bound any special moderators that might be present. The water-polyethylene mixture is considered bounding of all types of waste; therefore, there are no restrictions or requirements on the specific makeup of the waste form outside of the fissile material, beryllium, and B_4C content. The waste form modeled in this analysis is a mixture of 75% water and 25% polyethylene (modeled as CH_2). Variations of 100% water and 100% polyethylene were also considered for comparison. The amount of fissile material per container is 380 FGE ^{239}Pu, modeled as PuO_2, mixed homogeneously with the other materials. The total amount of the water/polyethylene mixture per container is varied to determine the optimum moderation to fissile material (H/Pu) ratio.

For closure scenarios, a neutron absorber is added to the models in order to ensure subcriticality. The neutron absorber is modeled as different amounts of B_4C in support of process optimization considerations, with the boron content considered as natural boron (19.9 wt% ^{10}B, 80.1wt% ^{11}B).

Other waste containers typically allow beryllium to be included for up to 1% by weight of the waste content [1, 2, 3], and may also be present in oxide form. As listed in [2], the empty weight for a criticality control overpack (CCO) was 104.3 kg (230 lb), with a maximum gross weight of 158.8 kg (350 lb), which resulted in a maximum waste weight of 54.5 kg. The beryllium content (1% by weight) is based on the total allowed waste weight (does not include packaging and container weights). Therefore, the 1%-by-weight limit for beryllium was determined to be 545 g, which is consistent with other container limits. Cases were run with 545 g of beryllium per CCO intermixed in the waste form.

Figure A-1 is a screenshot of a spreadsheet example demonstrating how the material weight percentages were determined for the calculational inputs.

Pu	**380**	g	H2O	amu	number per	w/o	CH2	amu	number per	w/o					
	19.84	g/cc	H	1.0078	2	0.1119	C	12.0107	1	0.8563					
	19.15323	cm3	O	15.9949	1	0.8881	H	1.0078	2	0.1437					
	239.0522	amu	sum	18.0105	g/mole		sum	14.0263	g/mole						
	1.589611	moles	density	0.9982	g/cc		density	0.92	g/cc						
PuO2	430.851337	g	**% H2O**	**0.75**			**% CH2**	**0.25**							
O	50.851337	g													
			PuO2	amu	number per	w/o	B4C	amu	number per	w/o					
Be	**545**	g	Pu	239.0522	1	0.8820	B	10.811	4	0.78					
	1.85	g/cc	O	15.9949	2	0.1180	C	12.0107	1	0.22					
	9.0122	amu	sum	271.042			sum	55.2547							
			density	11.46	g/cc		density	2.5	g/cc						
H/X	**200**			grams	w/o			**Composition**							**full collapse**
H moles	317.92219		H	320.40199	0.085887	1001	H	**1001**	**0.08589**	**H**					
			C	488.17700	0.130861	6000	C	**6000**	**0.13086**	**C**	fm height	16.6809		**0**	
H from H2O	238.44165		O	1957.77648	0.524805	8016	O	**8016**	**0.52480**	**O**	flange	2.54		**2.54**	
H2O moles	119.22082		Pu	380	0.101863	94239	Pu	**94239**	**0.10186**	**Pu**	flange	2.54		**19.2209**	
H2O grams	2147.22663	g	Be	545	0.146094	4000	Be	**4000**	**0.14609**	**Be**	total ht	21.7609		**21.7609**	
H2O cm3	2151.09861	cm3	B	39.13151	0.010490	5000	B	**5000**	**0.01049**	**B**					
H	240.30149	g		3730.48698	1.000000				1.0000		x3	65.2827	x3	65.283	
O	1906.92514	g						total density	**1.1998**	**g/cc**	round up	**65**	round up	**65**	
			Total		frac of total	ind dens									
H from CH2	79.48055		PuO2	430.85134	0.115495	11.46		total grams	**3730.4870**	**g**					
CH2 moles	39.74027		H2O	2147.22663	0.575589	0.9982									
CH2 grams	557.40901	g	CH2	557.40901	0.149420	0.92		total volume	**3109.1687**	**cc**					
CH3 cm3	605.87936	cm3	Be	545	0.146094	1.85									
C	477.30851	g	B4C	50	0.013403	2.5		Cylinder filling inside diameter			Sphere				
H	80.10050	g		3730.48698	1			radius	**7.7026**	**cm**	radius	**9.0542**	cm		
								height	**16.6809**	**cm**	Dr Center	upper h	lower h		
B4C	**50**	g	mix density	1.19983				h div by 2	8.3405		36.757	**45.0975**	**28.4165**		
B	39.13151	g						total inner ht	68.434						
C	10.86849	g						unfilled space	51.7531						
								divided by 2	**25.8765**	**cm**					

Figure A-1. Screenshot of spreadsheet determining generic waste composition.

A.2 BRINE IN FLOODED CONFIGURATIONS

The only significant source of water is from brine-filled fractures in rock units below and/or around the repository, from saturated clay seams near the repository, or from drilling fluid resulting from a hypothetical drilling event.

The brine would include other materials in addition to salt [4, 5] for various brine elemental concentrations in the WIPP area. The stew-like mixture would contain even more materials/elements from the structural/material degradation. The exact nature and amounts of these contaminants are difficult to quantify, so developing a bounding model is also difficult. Conservatively, the cases in this effort only modeled water with salt. The brine composition modeled is a representation of equilibrated brine based on the geochemistry of the area [5]. Reference [5] lists two equilibrated brine concentrations. The chlorine in the salt is expected to act as a neutron absorber and lower the multiplication of the system. Therefore, the lower equilibrated brine chlorine composition, with a molality of 5.98 mol (moles/kg of H_2O), was modeled here. Screenshots of the spreadsheet used to determine the number densities are shown in Figure A-2.

salt (halite) in water			
	grams per	density	
	mole	g/cm3	
H	1.0079		
O	15.9994		
H2O	18.0152	0.9982	
			wt %
Na	22.9898		0.3934
Cl	35.453		0.6066
NaCl	58.4428	2.165	

								density				
NaCl	NaCl	H2O	H2O	H2O	Total	Total	Total	total g/				
grams	cm3	liter	cm3	g	g	cm3	liter	total cm3				
349	161.2009	1	1000	998.2	1347	1161.2009	1.1612	1.1602	N(NaCl)	0.0030969	**N(Na)**	**0.003097**
											N(Cl)	**0.003097**
									N(H2O)	0.028735	**N(H)**	**0.057470**
											N(O)	**0.028735**

					molarity (M)		molality (m)				
					M		m				
			g NaCl	NaCl	moles/liter		moles/kg of solvent				
			per mole	moles	(total liters)		(kg of H2O)				
N(Na)	**0.003097**		58.4428	5.9717	**5.143**		5.98		ERDA-6, equilibrated (synthetic Castile)		
N(Cl)	**0.003097**										
N(H)	**0.057470**										
N(O)	**0.028735**										

Figure A-2. Screenshots of spreadsheet determining brine compositions.

A.3 REFERENCES

[1] DOE CBFO. 2013. *TRUPACT-II Safety Analysis Report*, Revision 23, US Department of Energy, Carlsbad Field Office, Carlsbad, New Mexico.

[2] DOE-CBFO. 2013. *Contact-Handled Transuranic Waste Authorized Methods for Payload Control (CH-TRAMPAC)*, Revision 4, US Department of Energy, Carlsbad Field Office, Carlsbad, New Mexico.

[3] DOE-CBFO. 2013. *CH-TRU Payload Appendices*, Revision 3, US Department of Energy, Carlsbad Field Office, Carlsbad, New Mexico.

[4] R. Rechard, L. Sanchez, C. Stockman, Holly T. 2000. *Consideration of Nuclear Criticality When Disposing of Transuranic Waste at the Waste Isolation Pilot Plant,* SAND99-2898, Sandia National Laboratories, Albuquerque, New Mexico.

[5] SNL. 2008. *Preparing Synthetic Brines for Geochemical Experiments*, Rev. 2, Activity/Project Specific Procedures, SP 20-4, Carlsbad, New Mexico: Sandia National Laboratories.

APPENDIX B. RESULTS

Table B.1 lists the data used to generate the figures in the body of this report. Tables are arranged by figure with each table containing case descriptions with the varying parameters identified. Peak k-effective values (k_{eff}s), ranging from 0.80 to 0.85, tend to have an H/Pu ratio of 200 to 400, with EALFs of about 0.42. Some scenarios have peak k-effective values (k_{eff}s) with higher H/Pu ratios and lower EALFs; however they are not considered bounding cases with their respective k_{eff}s lower than 0.80.

Table B-1. Data for Figures ES-1 and 6.

Legend entry on figure Case	Description	H/Pu	k_{eff}	sigma	$k_{eff} + 2\sigma$	EALF
full radial compaction, infinite						
g380infgenhx0100b050rd20vdcc	Infinite array, varying H/Pu, 50 g B_4C per CCO, full radial compaction	100	0.76797	0.00010	0.76816	1.21809
g380infgenhx0200b050rd20vdcc		**200**	0.82529	0.00010	**0.82549**	**0.42457**
g380infgenhx0300b050rd20vdcc		**300**	0.82852	0.00009	**0.82870**	**0.26286**
g380infgenhx0400b050rd20vdcc		400	0.81734	0.00009	0.81751	0.19522
g380infgenhx0500b050rd20vdcc		500	0.80083	0.00008	0.80099	0.15837
g380infgenhx0600b050rd20vdcc		600	0.78523	0.00007	0.78537	0.13504
g380infgenhx0700b050rd20vdcc		700	0.76865	0.00008	0.76880	0.11913
g380infgenhx0800b050rd20vdcc		800	0.75281	0.00008	0.75296	0.10748
g380infgenhx0895b050rd20vdcc		895	0.73553	0.00007	0.73567	0.09924
full radial compaction, room						
g380rmgenhx0100b050rd20vdcc	Room array, varying H/Pu, 50 g B_4C per CCO, full radial compaction	100	0.72377	0.00008	0.72392	1.24552
g380rmgenhx0200b050rd20vdcc		200	0.79903	0.00008	**0.79919**	**0.42759**
g380rmgenhx0300b050rd20vdcc		**300**	0.81120	0.00009	**0.81138**	**0.26378**
g380rmgenhx0400b050rd20vdcc		400	0.80509	0.00006	**0.80521**	**0.19560**
g380rmgenhx0500b050rd20vdcc		500	0.79308	0.00007	**0.79322**	**0.15838**
g380rmgenhx0600b050rd20vdcc		600	0.77882	0.00006	0.77894	0.13513
g380rmgenhx0700b050rd20vdcc		700	0.76299	0.00007	0.76312	0.11921
g380rmgenhx0800b050rd20vdcc		800	0.74839	0.00005	0.74850	0.10755
g380rmgenhx0895b050rd20vdcc		895	0.73429	0.00006	0.73440	0.09920
full radius, infinite						
g380infgenhx0100b050rdfrvdcc	Infinite array, varying H/Pu, 50 g B_4C per CCO, full radius (no compaction)	100	0.45966	0.00012	0.45990	1.40873
g380infgenhx0200b050rdfrvdcc		200	0.58091	0.00013	0.58117	0.44959
g380infgenhx0300b050rdfrvdcc		300	0.62722	0.00011	0.62744	0.27219
g380infgenhx0400b050rdfrvdcc		400	0.64637	0.00011	0.64659	0.20032
g380infgenhx0500b050rdfrvdcc		500	0.65090	0.00010	0.65110	0.16177
g380infgenhx0600b050rdfrvdcc		600	0.65461	0.00010	0.65481	0.13744
g380infgenhx0700b050rdfrvdcc		700	0.65200	0.00009	0.65219	0.12099
g380infgenhx0800b050rdfrvdcc		800	0.64829	0.00009	0.64847	0.10895
g380infgenhx0895b050rdfrvdcc		895	0.63338	0.00009	0.63355	0.10059
full radius, room						
g380rmgenhx0100b050rdfrvdcc	Room array, varying H/Pu, 50 g B_4C per CCO, full radius (no compaction)	100	0.40966	0.00009	0.40983	1.51608
g380rmgenhx0200b050rdfrvdcc		200	0.53433	0.00010	0.53453	0.46160
g380rmgenhx0300b050rdfrvdcc		300	0.58531	0.00008	0.58548	0.27637
g380rmgenhx0400b050rdfrvdcc		400	0.60880	0.00008	0.60896	0.20229
g380rmgenhx0500b050rdfrvdcc		500	0.61943	0.00007	0.61958	0.16278
g380rmgenhx0600b050rdfrvdcc		600	0.62488	0.00009	0.62505	0.13822
g380rmgenhx0700b050rdfrvdcc		700	0.62406	0.00007	0.62419	0.12164
g380rmgenhx0800b050rdfrvdcc		800	0.62261	0.00008	0.62276	0.10947
g380rmgenhx0895b050rdfrvdcc		895	0.61932	0.00007	0.61946	0.10078

Table B-2. Data for Figures ES-2 and 8.

Legend entry on figure Case	Description	B_4C (grams)	k_{eff}	sigma	$k_{eff} + 2\sigma$	EALF
full radial compaction						
g380rmgenhx0200rd20vdcc	Room array, H/Pu of 200, varying B_4C per CCO, full radial compaction	0	1.46694	0.00015	1.46724	0.16768
g380rmgenhx0200b025rd20vdcc		25	1.01534	0.00009	1.01551	0.29107
g380rmgenhx0200b050rd20vdcc		**50**	0.79903	0.00008	**0.79919**	**0.42759**
g380rmgenhx0200b100rd20vdcc		100	0.57151	0.00005	0.57161	0.75325
g380rmgenhx0200b150rd20vdcc		150	0.44657	0.00005	0.44666	1.18309
g380rmgenhx0200b200rd20vdcc		200	0.36636	0.00004	0.36645	1.76112
radius reduced by 14 cm						
g380rmgenhx0200rd14vdcc	Room array, H/Pu of 200, varying B_4C per CCO, CCO radius reduced by 14 cm	0	1.26807	0.00014	1.26835	0.17168
g380rmgenhx0200b025rd14vdcc		25	0.88192	0.00010	0.88213	0.29846
g380rmgenhx0200b050rd14vdcc		50	0.69622	0.00008	0.69639	0.43864
g380rmgenhx0200b100rd14vdcc		100	0.50052	0.00007	0.50065	0.77295
g380rmgenhx0200b150rd14vdcc		150	0.39256	0.00005	0.39267	1.21303
g380rmgenhx0200b200rd14vdcc		200	0.32303	0.00004	0.32312	1.80343
radius reduced by 7 cm						
g380rmgenhx0200rd07vdcc	Room array, H/Pu of 200, varying B_4C per CCO, CCO radius reduced by 7 cm	0	1.09936	0.00016	1.09968	0.17461
g380rmgenhx0200b025rd07vdcc		25	0.76552	0.00011	0.76574	0.30481
g380rmgenhx0200b050rd07vdcc		50	0.60515	0.00010	0.60535	0.44947
g380rmgenhx0200b100rd07vdcc		100	0.43617	0.00007	0.43630	0.79581
g380rmgenhx0200b150rd07vdcc		150	0.34298	0.00005	0.34309	1.25338
g380rmgenhx0200b200rd07vdcc		200	0.28281	0.00005	0.28291	1.86678
full radius						
g380rmgenhx0200rdfrvdcc	Room array, H/Pu of 200, varying B_4C per CCO, full radius (no compaction)	0	0.97011	0.00018	0.97047	0.17729
g380rmgenhx0200b025rdfrvdcc		25	0.67556	0.00011	0.67578	0.31160
g380rmgenhx0200b050rdfrvdcc		50	0.53433	0.00010	0.53453	0.46160
g380rmgenhx0200b100rdfrvdcc		100	0.38568	0.00006	0.38581	0.82336
g380rmgenhx0200b150rdfrvdcc		150	0.30377	0.00005	0.30388	1.30273
g380rmgenhx0200b200rdfrvdcc		200	0.25094	0.00004	0.25103	1.94959

Table B-3. Data for Figure 9

Legend entry on figure Case	Description	B_4C (grams)	k_{eff}	sigma	$k_{eff} + 2\sigma$	EALF
H/Pu of 100						
g380rmgenhx0100b025rd20vdcc	Room array, H/Pu of 100, varying B_4C per CCO, full radial compaction	25	0.92875	0.00010	0.92895	0.75359
g380rmgenhx0100b050rd20vdcc		50	0.72377	0.00008	0.72392	1.24552
g380rmgenhx0100b100rd20vdcc		100	0.50713	0.00005	0.50724	2.78162
g380rmgenhx0100b150rd20vdcc		150	0.39265	0.00005	0.39275	5.44041
g380rmgenhx0100b200rd20vdcc		200	0.32266	0.00004	0.32274	9.71412
H/Pu of 200						
g380rmgenhx0200b025rd20vdcc	Room array, H/Pu of 200, varying B_4C per CCO, full radial compaction	25	1.01534	0.00009	1.01551	0.29107
g380rmgenhx0200b050rd20vdcc		**50**	0.79903	0.00008	**0.79919**	**0.42759**
g380rmgenhx0200b100rd20vdcc		100	0.57151	0.00005	0.57161	0.75325
g380rmgenhx0200b150rd20vdcc		150	0.44657	0.00005	0.44666	1.18309
g380rmgenhx0200b200rd20vdcc		200	0.36636	0.00004	0.36645	1.76112
H/Pu of 300						
g380rmgenhx0300b025rd20vdcc	Room array, H/Pu of 300, varying B_4C per CCO, full radial compaction	25	1.02872	0.00009	1.02890	0.18744
g380rmgenhx0300b050rd20vdcc		**50**	0.81120	0.00009	**0.81138**	**0.26378**
g380rmgenhx0300b100rd20vdcc		100	0.58663	0.00005	0.58674	0.43048
g380rmgenhx0300b150rd20vdcc		150	0.46429	0.00004	0.46438	0.62313
g380rmgenhx0300b200rd20vdcc		200	0.38455	0.00004	0.38463	0.85315
H/Pu of 400						
g380rmgenhx0400b025rd20vdcc	Room array, H/Pu of 400, varying B_4C per CCO, full radial compaction	25	1.02169	0.00008	1.02185	0.14281
g380rmgenhx0400b050rd20vdcc		**50**	0.80509	0.00006	**0.80521**	**0.19560**
g380rmgenhx0400b100rd20vdcc		100	0.58504	0.00005	0.58515	0.30727
g380rmgenhx0400b150rd20vdcc		150	0.46674	0.00004	0.46682	0.42835
g380rmgenhx0400b200rd20vdcc		200	0.38972	0.00004	0.38980	0.56359
H/Pu of 500						
g380rmgenhx0500b025rd20vdcc	Room array, H/Pu of 500, varying B_4C per CCO, full radial compaction	25	1.00637	0.00008	1.00653	0.11829
g380rmgenhx0500b050rd20vdcc		50	0.79308	0.00007	0.79322	0.15838
g380rmgenhx0500b100rd20vdcc		100	0.57719	0.00005	0.57729	0.24253
g380rmgenhx0500b150rd20vdcc		150	0.46267	0.00004	0.46276	0.33104
g380rmgenhx0500b200rd20vdcc		200	0.38827	0.00004	0.38834	0.42609
H/Pu of 600						
g380rmgenhx0600b025rd20vdcc	Room array, H/Pu of 600, varying B_4C per CCO, full radial compaction	25	0.98730	0.00008	0.98745	0.10288
g380rmgenhx0600b050rd20vdcc		50	0.77882	0.00006	0.77894	0.13513
g380rmgenhx0600b100rd20vdcc		100	0.56710	0.00005	0.56719	0.20248
g380rmgenhx0600b150rd20vdcc		150	0.45565	0.00004	0.45573	0.27266
g380rmgenhx0600b200rd20vdcc		200	0.38402	0.00004	0.38410	0.34599
H/Pu of 700						
g380rmgenhx0700b025rd20vdcc	Room array, H/Pu of 700, varying B_4C per CCO, full radial compaction	25	0.96779	0.00007	0.96793	0.09224
g380rmgenhx0700b050rd20vdcc		50	0.76299	0.00007	0.76312	0.11921
g380rmgenhx0700b100rd20vdcc		100	0.55665	0.00004	0.55673	0.17528
g380rmgenhx0700b150rd20vdcc		150	0.44801	0.00004	0.44810	0.23335
g380rmgenhx0700b200rd20vdcc		200	0.37842	0.00003	0.37849	0.29345
H/Pu of 800						
g380rmgenhx0800b025rd20vdcc	Room array, H/Pu of 800, varying B_4C per CCO, full radial compaction	25	0.94760	0.00007	0.94774	0.08457
g380rmgenhx0800b050rd20vdcc		50	0.74839	0.00005	0.74850	0.10755
g380rmgenhx0800b100rd20vdcc		100	0.54586	0.00004	0.54595	0.15567
g380rmgenhx0800b150rd20vdcc		150	0.43975	0.00005	0.43984	0.20527
g380rmgenhx0800b200rd20vdcc		200	0.37225	0.00003	0.37231	0.25617
H/Pu of 895						
g380rmgenhx0895b025rd20vdcc	Room array, H/Pu of 895, varying B_4C per CCO, full radial compaction	25	0.93009	0.00007	0.93023	0.07885
g380rmgenhx0895b050rd20vdcc		50	0.73429	0.00006	0.73440	0.09920
g380rmgenhx0895b100rd20vdcc		100	0.53601	0.00004	0.53610	0.14144
g380rmgenhx0895b150rd20vdcc		150	0.43229	0.00004	0.43237	0.18490
g380rmgenhx0895b200rd20vdcc		200	0.36617	0.00003	0.36622	0.22960

Table B-4. Data for Figure 10

Legend entry on figure Case	Description	H/Pu	k_{eff}	sigma	$k_{eff} + 2\sigma$	EALF
infinite, brine outside						
g380infgenhx0100b050rd20vdccbo	Infinite array, varying H/Pu, 50 g B_4C per CCO, full radial compaction, brine outside of CCO	100	0.55741	0.00013	0.55767	1.01464
g380infgenhx0200b050rd20vdccbo		200	0.68099	0.00011	0.68121	0.38976
g380infgenhx0300b050rd20vdccbo		300	0.72191	0.00011	0.72213	0.24761
g380infgenhx0400b050rd20vdccbo		**400**	0.73263	0.00010	**0.73283**	**0.18634**
g380infgenhx0500b050rd20vdccbo		500	0.72821	0.00009	0.72839	0.15229
g380infgenhx0600b050rd20vdccbo		600	0.72208	0.00010	0.72227	0.13070
g380infgenhx0700b050rd20vdccbo		700	0.71099	0.00009	0.71116	0.11591
g380infgenhx0800b050rd20vdccbo		800	0.69951	0.00008	0.69967	0.10500
g380infgenhx0895b050rd20vdccbo		895	0.68493	0.00009	0.68510	0.09732
room, brine outside						
g380rmgenhx0100b050rd20vdccbo	Room array, varying H/Pu, 50 g B_4C per CCO, full radial compaction, brine outside of CCO	100	0.54261	0.00009	0.54279	1.03203
g380rmgenhx0200b050rd20vdccbo		200	0.67100	0.00009	0.67119	0.39159
g380rmgenhx0300b050rd20vdccbo		300	0.71509	0.00008	0.71526	0.24817
g380rmgenhx0400b050rd20vdccbo		400	0.72689	0.00008	0.72704	0.18648
g380rmgenhx0500b050rd20vdccbo		500	0.72580	0.00007	0.72594	0.15232
g380rmgenhx0600b050rd20vdccbo		600	0.71856	0.00007	0.71869	0.13079
g380rmgenhx0700b050rd20vdccbo		700	0.70752	0.00007	0.70766	0.11593
g380rmgenhx0800b050rd20vdccbo		800	0.69647	0.00006	0.69659	0.10502
g380rmgenhx0895b050rd20vdccbo		895	0.68499	0.00006	0.68511	0.09719
infinite, brine everywhere						
g380infgenhx0100b050rd20vdccbe	Infinite array, varying H/Pu, 50 g B_4C per CCO, full radial compaction, brine everywhere (inside and outside of CCO)	100	0.48807	0.00012	0.48831	0.93052
g380infgenhx0200b050rd20vdccbe		200	0.62982	0.00013	0.63008	0.37733
g380infgenhx0300b050rd20vdccbe		300	0.68560	0.00013	0.68586	0.24315
g380infgenhx0400b050rd20vdccbe		400	0.70535	0.00011	0.70557	0.18395
g380infgenhx0500b050rd20vdccbe		500	0.70610	0.00011	0.70632	0.15081
g380infgenhx0600b050rd20vdccbe		600	0.70449	0.00010	0.70469	0.12974
g380infgenhx0700b050rd20vdccbe		700	0.69652	0.00010	0.69672	0.11502
g380infgenhx0800b050rd20vdccbe		800	0.68901	0.00010	0.68921	0.10416
g380infgenhx0895b050rd20vdccbe		895	0.68436	0.00008	0.68452	0.09714
room, brine everywhere						
g380rmgenhx0100b050rd20vdccbe	Room array, varying H/Pu, 50 g B_4C per CCO, full radial compaction, brine everywhere (inside and outside of CCO)	100	0.48628	0.00010	0.48647	0.93335
g380rmgenhx0200b050rd20vdccbe		200	0.62753	0.00009	0.62770	0.37763
g380rmgenhx0300b050rd20vdccbe		300	0.68316	0.00010	0.68335	0.24326
g380rmgenhx0400b050rd20vdccbe		400	0.70268	0.00009	0.70286	0.18406
g380rmgenhx0500b050rd20vdccbe		500	0.70633	0.00007	0.70647	0.15086
g380rmgenhx0600b050rd20vdccbe		600	0.70227	0.00008	0.70243	0.12974
g380rmgenhx0700b050rd20vdccbe		700	0.69352	0.00007	0.69365	0.11507
g380rmgenhx0800b050rd20vdccbe		800	0.68616	0.00006	0.68627	0.10420
g380rmgenhx0895b050rd20vdccbe		895	0.68447	0.00006	0.68458	0.09705

Table B-5. Data for Figure 12.

Legend entry on figure Case	Description	H/Pu	k_{eff}	sigma	$k_{eff} + 2\sigma$	EALF
infinite, no brine						
g380infgenhx0100b050rd20vdfc	Infinite array, varying H/Pu, 50 g B_4C per CCO, full radial compaction, full vertical compaction (full collapse)	100	0.80793	0.00009	0.80812	1.19443
g380infgenhx0200b050rd20vdfc		**200**	0.84985	0.00009	**0.85003**	**0.42140**
g380infgenhx0300b050rd20vdfc		300	0.84478	0.00009	**0.84496**	**0.26172**
g380infgenhx0400b050rd20vdfc		400	0.82839	0.00009	0.82857	0.19463
g380infgenhx0500b050rd20vdfc		500	0.80848	0.00008	0.80864	0.15804
g380infgenhx0600b050rd20vdfc		600	0.79013	0.00007	0.79028	0.13490
g380infgenhx0700b050rd20vdfc		700	0.77136	0.00009	0.77153	0.11903
g380infgenhx0800b050rd20vdfc		800	0.75412	0.00008	0.75427	0.10743
g380infgenhx0895b050rd20vdfc		895	0.73810	0.00009	0.73828	0.09913
room, no brine						
g380rmgenhx0100b050rd20vdfc	Room array, varying H/Pu, 50 g B_4C per CCO, full radial compaction, full vertical compaction (full collapse)	100	0.79950	0.00008	0.79965	1.20113
g380rmgenhx0200b050rd20vdfc		200	0.84364	0.00008	**0.84380**	**0.42192**
g380rmgenhx0300b050rd20vdfc		300	0.83945	0.00007	**0.83958**	**0.26204**
g380rmgenhx0400b050rd20vdfc		400	0.82358	0.00006	0.82369	0.19486
g380rmgenhx0500b050rd20vdfc		500	0.80511	0.00006	0.80523	0.15798
g380rmgenhx0600b050rd20vdfc		600	0.78586	0.00006	0.78598	0.13494
g380rmgenhx0700b050rd20vdfc		700	0.76742	0.00006	0.76754	0.11910
g380rmgenhx0800b050rd20vdfc		800	0.75036	0.00006	0.75047	0.10749
g380rmgenhx0895b050rd20vdfc		895	0.73433	0.00006	0.73445	0.09919
infinite, brine everywhere						
g380infgenhx0100b050rd20vdfcbo	Infinite array, varying H/Pu, 50 g B_4C per CCO, full radial compaction, full vertical compaction (full collapse), brine everywhere	100	0.75366	0.00010	0.75386	1.03741
g380infgenhx0200b050rd20vdfcbo		200	0.79479	0.00010	0.79499	0.39144
g380infgenhx0300b050rd20vdfcbo		300	0.79020	0.00010	0.79039	0.24854
g380infgenhx0400b050rd20vdfcbo		400	0.77445	0.00009	0.77464	0.18686
g380infgenhx0500b050rd20vdfcbo		500	0.75477	0.00009	0.75495	0.15278
g380infgenhx0600b050rd20vdfcbo		600	0.73792	0.00009	0.73811	0.13103
g380infgenhx0700b050rd20vdfcbo		700	0.72002	0.00008	0.72018	0.11609
g380infgenhx0800b050rd20vdfcbo		800	0.70346	0.00009	0.70363	0.10513
g380infgenhx0895b050rd20vdfcbo		895	0.68819	0.00008	0.68835	0.09718
room, brine everywhere						
g380rmgenhx0100b050rd20vdfcbo	Room array, varying H/Pu, 50 g B_4C per CCO, full radial compaction, full vertical compaction (full collapse), brine everywhere	100	0.74720	0.00008	0.74735	1.04199
g380rmgenhx0200b050rd20vdfcbo		200	0.78974	0.00008	0.78990	0.39216
g380rmgenhx0300b050rd20vdfcbo		300	0.78596	0.00008	0.78613	0.24879
g380rmgenhx0400b050rd20vdfcbo		400	0.77087	0.00007	0.77100	0.18704
g380rmgenhx0500b050rd20vdfcbo		500	0.75294	0.00006	0.75307	0.15273
g380rmgenhx0600b050rd20vdfcbo		600	0.73450	0.00007	0.73464	0.13106
g380rmgenhx0700b050rd20vdfcbo		700	0.71683	0.00006	0.71695	0.11613
g380rmgenhx0800b050rd20vdfcbo		800	0.70037	0.00006	0.70049	0.10511
g380rmgenhx0895b050rd20vdfcbo		895	0.68522	0.00006	0.68534	0.09719

Table B-6. Data for Table 2.

Case	Description	k_{eff}	sigma	$k_{eff} + 2\sigma$	EALF
For reference					
g380rmgenhx0200b050rdfrvdcc	Room array (3 tier), H/Pu of 200, 50 g B_4C per CCO, **full radius (no compaction)**	0.53433	0.00010	0.53453	0.46160
g380rmgenhx0200b050rd20vdfc	Room array, H/Pu of 200, 50 g B_4C per CCO, full radial and vertical compaction	0.84364	0.00008	**0.84380**	**0.42192**
3rd tier combined with 2nd tier					
g380rmgenhx0200b050rdvarvdfc_2high_fr	Room array (3 tier), H/Pu of 200, 50 g B_4C per CCO, bottom tier with no radial compaction	0.77330	0.00008	0.77345	0.42392
g380rmgenhx0200b050rdvarvdfc_2high_rd119	Room array, H/Pu of 200, 50 g B_4C per CCO, bottom tier radially compacted to combined tier width	0.78431	0.00007	0.78445	0.42442
g380rmgenhx0200b050rd20vdfc_2high_rd20	Room array, H/Pu of 200, 50 g B_4C per CCO, bottom tier with full radial compaction	0.82290	0.00007	0.82303	0.42198
3rd tier split between 2nd and 1st tier					
g380rmgenhx0200b050rd10vdfc_2high_equal	Room array, H/Pu of 200, 50 g B_4C per CCO, radially compacted to original room width	0.65443	0.00010	0.65443	0.43699
g380rmgenhx0200b050rd20vdfc_2high_equal	Room array, H/Pu of 200, 50 g B_4C per CCO, full radial compaction	0.82593	0.00007	0.82593	0.42182

Table B-7. Data for Figure 13.

Legend entry on figure Case	Description	H/Pu	k_{eff}	sigma	$k_{eff} + 2\sigma$	EALF
100% polyethylene, double density						
g380rmpol2hx0100b050rd20vdfc		100	0.81126	0.00007	0.81141	1.18219
g380rmpol2hx0200b050rd20vdfc		**200**	0.86157	0.00007	**0.86172**	**0.41330**
g380rmpol2hx0300b050rd20vdfc		**300**	0.86270	0.00006	**0.86283**	**0.25510**
g380rmpol2hx0400b050rd20vdfc		400	0.85103	0.00007	0.85116	0.18885
g380rmpol2hx0500b050rd20vdfc		500	0.83588	0.00006	0.83600	0.15271
g380rmpol2hx0600b050rd20vdfc		600	0.82040	0.00006	0.82052	0.12992
g380rmpol2hx0700b050rd20vdfc		700	0.80501	0.00005	0.80512	0.11432
g380rmpol2hx0800b050rd20vdfc		800	0.78986	0.00006	0.78998	0.10309
g380rmpol2hx0900b050rd20vdfc	Room array,	900	0.77629	0.00006	0.77641	0.09447
g380rmpol2hx1000b050rd20vdfc	waste mix is 100%	1000	0.76358	0.00005	0.76368	0.08771
g380rmpol2hx1100b050rd20vdfc	polyethylene at double density,	1100	0.75123	0.00005	0.75134	0.08233
g380rmpol2hx1200b050rd20vdfc	varying H/Pu,	1200	0.73842	0.00005	0.73851	0.07799
g380rmpol2hx1300b050rd20vdfc	50 g B_4C per CCO,	1300	0.72773	0.00005	0.72783	0.07425
g380rmpol2hx1400b050rd20vdfc	full radial compaction,	1400	0.71713	0.00006	0.71724	0.07113
g380rmpol2hx1500b050rd20vdfc		1500	0.70706	0.00004	0.70715	0.06843
g380rmpol2hx1600b050rd20vdfc		1600	0.69707	0.00006	0.69718	0.06612
g380rmpol2hx1700b050rd20vdfc		1700	0.68678	0.00005	0.68688	0.06416
g380rmpol2hx1800b050rd20vdfc		1800	0.67702	0.00004	0.67710	0.06241
g380rmpol2hx1900b050rd20vdfc		1900	0.66913	0.00005	0.66923	0.06076
g380rmpol2hx2000b050rd20vdfc		2000	0.65973	0.00005	0.65983	0.05937
g380rmpol2hx2100b050rd20vdfc		2100	0.65214	0.00005	0.65224	0.05808
g380rmpol2hx2200b050rd20vdfc		2200	0.64411	0.00005	0.64420	0.05693
g380rmpol2hx2225b050rd20vdfc		2225	0.64281	0.00005	0.64290	0.05663
100% polyethylene						
g380rmpolhx0100b050rd20vdfc		100	0.80319	0.00008	0.80334	1.18866
g380rmpolhx0200b050rd20vdfc		**200**	0.84862	0.00008	**0.84877**	**0.41799**
g380rmpolhx0300b050rd20vdfc	Room array,	**300**	0.84549	0.00007	**0.84563**	**0.25934**
g380rmpolhx0400b050rd20vdfc	waste mix is 100%	400	0.83037	0.00007	0.83051	0.19273
g380rmpolhx0500b050rd20vdfc	polyethylene,	500	0.81199	0.00006	0.81210	0.15633
g380rmpolhx0600b050rd20vdfc	varying H/Pu,	600	0.79403	0.00006	0.79414	0.13334
g380rmpolhx0700b050rd20vdfc	50 g B_4C per CCO,	700	0.77605	0.00006	0.77616	0.11763
g380rmpolhx0800b050rd20vdfc	full radial compaction,	800	0.75857	0.00007	0.75872	0.10627
g380rmpolhx0900b050rd20vdfc		900	0.74290	0.00006	0.74301	0.09755
g380rmpolhx1000b050rd20vdfc		1000	0.72834	0.00006	0.72846	0.09069
g380rmpolhx1023b050rd20vdfc		1023	0.72443	0.00005	0.72453	0.08941
100% water						
g380rmwathx0100b050rd20vdfc		100	0.79834	0.00007	0.79848	1.20520
g380rmwathx0200b050rd20vdfc		**200**	0.84196	0.00007	**0.84209**	**0.42340**
g380rmwathx0300b050rd20vdfc	Room array,	300	0.83725	0.00007	**0.83738**	**0.26307**
g380rmwathx0400b050rd20vdfc	waste mix is 100% water,	400	0.82098	0.00006	0.82109	0.19572
g380rmwathx0500b050rd20vdfc	varying H/Pu,	500	0.80239	0.00007	0.80253	0.15867
g380rmwathx0600b050rd20vdfc	50 g B_4C per CCO,	600	0.78293	0.00006	0.78304	0.13551
g380rmwathx0700b050rd20vdfc	full radial compaction,	700	0.76483	0.00007	0.76498	0.11954
g380rmwathx0800b050rd20vdfc		800	0.74650	0.00006	0.74662	0.10808
g380rmwathx0860b050rd20vdfc		860	0.73731	0.00006	0.73743	0.10243

Table B-8. Data for Figure 14.

Legend entry on figure Case	Description	H/Pu	k_{eff}	sigma	$k_{eff} + 2\sigma$	EALF
full radial and vertical compaction						
g380rmgenhx0100b050rd20vdfcmgo	Room array, varying H/Pu, 50 g B_4C per CCO, full radial compaction, full vertical compaction (full collapse), MgO surrounding the CCOs	100	0.80111	0.00007	0.80125	1.19191
g380rmgenhx0200b050rd20vdfcmgo		**200**	0.84448	0.00007	**0.84462**	**0.42034**
g380rmgenhx0300b050rd20vdfcmgo		**300**	0.83988	0.00007	**0.84001**	**0.26132**
g380rmgenhx0400b050rd20vdfcmgo		400	0.82394	0.00006	0.82406	0.19441
g380rmgenhx0500b050rd20vdfcmgo		500	0.80535	0.00007	0.80548	0.15775
g380rmgenhx0600b050rd20vdfcmgo		600	0.78599	0.00006	0.78612	0.13472
g380rmgenhx0700b050rd20vdfcmgo		700	0.76753	0.00005	0.76764	0.11894
g380rmgenhx0800b050rd20vdfcmgo		800	0.75028	0.00006	0.75039	0.10736
g380rmgenhx0895b050rd20vdfcmgo		895	0.73443	0.00006	0.73454	0.09907
full radial compaction						
g380rmgenhx0100b050rd20vdccmgo	Room array, varying H/Pu, 50 g B_4C per CCO, full radial compaction, MgO surrounding the CCOs	100	0.72801	0.00008	0.72817	1.21709
g380rmgenhx0200b050rd20vdccmgo		200	0.80109	0.00007	**0.80123**	**0.42405**
g380rmgenhx0300b050rd20vdccmgo		**300**	0.81221	0.00009	**0.81238**	**0.26256**
g380rmgenhx0400b050rd20vdccmgo		400	0.80576	0.00006	**0.80589**	**0.19497**
g380rmgenhx0500b050rd20vdccmgo		500	0.79367	0.00007	0.79380	0.15801
g380rmgenhx0600b050rd20vdccmgo		600	0.77903	0.00007	0.77916	0.13487
g380rmgenhx0700b050rd20vdccmgo		700	0.76331	0.00007	0.76344	0.11902
g380rmgenhx0800b050rd20vdccmgo		800	0.74837	0.00006	0.74849	0.10740
g380rmgenhx0895b050rd20vdccmgo		895	0.73408	0.00006	0.73419	0.09905
no compaction						
g380rmgenhx0100b050rdfrvdccmgo	Room array, varying H/Pu, 50 g B_4C per CCO, full radius (no compaction), MgO surrounding the CCOs	100	0.40573	0.00009	0.40590	0.94761
g380rmgenhx0200b050rdfrvdccmgo		200	0.52091	0.00011	0.52113	0.37017
g380rmgenhx0300b050rdfrvdccmgo		300	0.57015	0.00009	0.57033	0.23712
g380rmgenhx0400b050rdfrvdccmgo		400	0.59371	0.00009	0.59389	0.17951
g380rmgenhx0500b050rdfrvdccmgo		500	0.60542	0.00008	0.60558	0.14733
g380rmgenhx0600b050rdfrvdccmgo		600	0.61143	0.00007	0.61157	0.12695
g380rmgenhx0700b050rdfrvdccmgo		700	0.61140	0.00008	0.61155	0.11288
g380rmgenhx0800b050rdfrvdccmgo		800	0.61042	0.00007	0.61056	0.10250
g380rmgenhx0895b050rdfrvdccmgo		895	0.60723	0.00008	0.60738	0.09503

APPENDIX C. ELECTRONIC FILES

The following spreadsheets contain the material composition derivations and dimensions used in the calculations.

Spreadsheet name:	**Description:**
NF Mix Composition.xlsx	Contains the waste form material composition and dimension derivations
k5 geom dec array sp w ccc struc.xlsx	Contains the dimension derivations for array geometries modeled in KENO V.a

The majority of the calculational files (input files ending in ".inp" and output files ending in ".out") are arranged in folders, with the folder name identifying the respective table in which the calculational results are reported. Included in each table folder is a summary text file (ending in ".dat") of the k_{eff} values and EALF (energy of average neutron lethargy causing fission) values. The validation calculational files are in the folder entitled *Validation*. The validation files include input and output files, sensitivity files (ending in ".sdf"), and the USLSTATS files (contained in folders ending in ".uslstats").

APPENDIX D. CALCULATIONAL VALIDATION

The calculations for this report were performed using the SCALE code system, version 6.2.3. The Criticality Safety Analysis Sequence (CSAS) with KENO V.a (CSAS5) was used to calculate effective neutron multiplication factors, or k-effective (k_{eff}) values, for the various scenarios analyzed. As with any computer code or calculation used in relation to safety analyses and assessments, the ability of the calculation methodology to prove a configuration subcritical is obtained through a validation process.

The validation process assesses how well a computational method predicts reality (e.g., whether a system that was calculated to be subcritical is in reality subcritical). Applicable industry standards, such as the American National Standards Institute (ANSI)/American Nuclear Society (ANS)-8 standards, *An American National Standard for Nuclear Criticality Safety in Operations with Fissionable Materials Outside Reactors*, ANSI/ANS-8.1-2014 [1], and *An American National Standard for Validation on Neutron Transport Methods for Nuclear Criticality Safety Calculations*, ANSI/ANS-8.24-2017 [2], require validation to be conducted through comparisons of computed results with experimental data. Typically, well-documented critical experiments (critical benchmarks) are used for these comparisons. Documented critical experiments can be found in a variety of resources, including the *International Handbook of Evaluated Criticality Safety Benchmark Experiments* [3]. Ideally, models of critical experiments would calculate results that are exactly equal to experimental results. In reality, calculational results do not exactly match experimental results because of simplifications and approximations made in the computational models to facilitate solutions on computer systems. Furthermore, the nuclear data used may include errors associated with the measurement, evaluation, and/or representation of the data. The validation process provides an understanding of the difference between calculated and experimental results, or *bias*, and the uncertainty in this difference, or *bias uncertainty*.

For a validation to yield an appropriate bias and bias uncertainty, the critical experiments used for comparison must be as similar as possible to the application being validated. Critical experiments are arrangements of fissile material and structural materials usually performed to support operational needs and processes. Validation of waste disposal operations can be challenging due to the difficulty in finding experiments similar in nature to waste disposal materials and operations.

The validation results (bias and bias uncertainty) are used to determine an upper subcritical limit (USL). Calculated results (including calculational uncertainty, $k_{eff\text{-calc}} + 2\sigma_{calc}$) below the USL are considered subcritical; results above the USL (even those below 1.0) are not considered to be subcritical. Determination of the USL can also include an additional margin of subcriticality to account for dissimilarities between the experiments used and the application and identified gaps in the nuclear data. The USL can be considered as the magnitude of the sum of the biases, uncertainties, and administrative and/or statistical margins applied to a set of critical benchmarks. Because a positive bias may be nonconservative, all positive biases are set to zero. An allowance to use a positive bias, if the cause of the positive bias is well understood and justified, has been established in [2], but is not typical. The USL can be represented by the following:

$$\text{USL} = 1.0 + \text{bias} - \text{bias uncertainty} - \text{administrative margin}$$

$$k_{eff\text{-calc}} + 2\sigma_{calc} < \text{USL}$$

Historically, the expected computational bias is established with the use of trending analyses of the bias for the critical experiments as a function of their physical characteristics such as H/X or energy of average neutron lethargy causing fission (EALF). The bias uncertainty is then determined through a statistical analysis of the trend, taking into account the uncertainty in each k_{eff} data point and the distribution of the data. The trending analysis can also be done with sensitivity/uncertainty (S/U) tools. The S/U tools are

used to determine correlation coefficients(c_k value or c(k)) for trending analysis. This report uses both c(k) and EALF values for trending analyses.

For the S/U method, the TSUNAMI sequence included in the SCALE code system was used to quantify the similarity of each selected critical experiment and application model pair. This technique provides a physics-based approach to benchmark critical experiment selection. The TSUNAMI methods are based on the premise that the primary source of computational biases are the errors in the cross section data as bounded by their uncertainties, which can be tabulated in cross section covariance data. The TSUNAMI-3D sequence was used to compute sensitivity data for the applications and for each selected critical experiment. The TSUNAMI-IP sequence was then used to compare the sensitivity data between the application and the critical experiments, giving greater weight to comparisons of sensitivities for nuclides and reactions with the highest nuclear data uncertainties. For each model, TSUNAMI-IP combined the sensitivity data and the cross section covariance data to generate nuclide-, reaction-, and energy-dependent k_{eff} uncertainty data. A correlation coefficient, c_k value or c(k), was calculated, indicating the degree to which each application and critical experiment model pair share k_{eff} uncertainty. A high c_k value (approaching one) would indicate that the two compared systems share a similar sensitivity to the same nuclear data uncertainty. Based on the assumption that computational biases are due primarily to nuclear data errors and that the nuclear data uncertainty values should indicate the potential for such nuclear data errors, two highly correlated systems should exhibit the same computational bias. The Upper Subcritical Limit Statistics (USLSTATS) program, a statistical analysis program distributed with SCALE, was then used to perform a trending analysis on the c(k) values and calculate the final bias, bias uncertainty, and resulting USL. USLSTATS was also used with the EALF values as the trending parameter for comparison.

For this analysis, the applications were the cases with the highest calculated system k_{eff}s, with consideration of both a dry and wet scenario. The criticality experiments chosen are from *The SCALE Verified, Archived Library of Inputs and Data—VALID* [4], with all of the chosen experiments also included in the *International Handbook of Evaluated Criticality Safety Benchmark Experiments* [3]. There were 81 experiments chosen from the plutonium-solution-thermal category (PST), 21 from the mixed-composition-thermal category (MCT), and 10 from the mixed-solution-thermal category (MST), with an EALF range of 0.04 to 0.95 eV. The experiments are similar to the applications in the ^{239}Pu content with an average of > 95% ^{239}Pu in the Pu content. The plutonium solution experiments are water moderated and are in the thermal energy region. The mixed composition and mixed solution experiments systems cover more of the upper thermal into intermediate energy regions. Most of the important isotopes from the application systems are included in the experiments chosen (e.g., hydrogen, boron, and carbon), the exceptions being beryllium and chlorine.

To account for the potential bias from the beryllium and chlorine, their respective nuclear data uncertainties were used to develop a bounding estimate of their bias. This methodology is described in *An Approach for Validating Actinide and Fission Product Burnup Credit Criticality Safety Analyses-Criticality (k_{eff}) Predictions* [5]. The sensitivity files generated by the TSUNAMI-3D sequence lists the uncertainty for each nuclide reaction. The total uncertainties for beryllium and chlorine are determined by combining the individual nuclide reaction uncertainties. This uncertainty is then combined with the bias and bias uncertainty determined by USLSTATS. Per Reference [5], three times the nuclear data uncertainty is a conservative bounding estimate for the bias.

D.1 RECONFIGURED DRY SCENARIO

For the dry scenario, the case chosen is g380infgenhx0200b050rd20vdcc, which has 50 g of B_4C and 545 g of beryllium into the waste form with a $k_{eff} + 2\sigma$ of 0.82549 and an EALF of 0.42 eV. The case is an infinite array with full radial compaction. The TSUNAMI-IP calculated c(k) values are provided in Table

D.1. From the compared critical experiments, the c(k) values ranged from 0.63 to 0.78. Ideally, benchmark experiments should have a c(k) greater than 0.8 to be considered for validation. However, experiments that model materials similar to this waste form do not exist.

Table D-1. Reconfigured dry scenario c(k) values.

Experiment	c(k) value	Experiment	c(k) value	Experiment	c(k) value	Experiment	c(k) value
MCT-002-004S	0.77	PST-005-007	0.66	PST-003-002	0.65	PST-007-005	0.64
MCT-002-006S	0.76	PST-005-001	0.66	PST-011-012	0.65	PST-007-004	0.64
MST-007-002	0.71	PST-004-007	0.66	PST-003-001	0.65	PST-007-008	0.64
MST-007-001	0.71	PST-004-009	0.66	PST-011-007	0.65	MCT-004-010	0.64
MCT-001-001	0.71	PST-020-002	0.66	PST-011-011	0.65	MCT-004-003	0.64
MCT-001-002	0.69	PST-020-009	0.66	PST-011-008	0.65	PST-007-006	0.64
MST-002-003	0.68	PST-004-008	0.66	PST-011-009	0.65	PST-007-007	0.64
MST-007-003	0.68	PST-004-012	0.66	PST-011-006	0.65	MCT-004-007	0.64
MCT-001-003	0.68	PST-004-013	0.66	PST-007-001	0.65	MCT-004-005	0.64
MCT-002-002S	0.68	PST-004-006	0.66	PST-002-005	0.65	PST-020-008	0.64
MST-002-001	0.68	PST-020-015	0.66	PST-002-004	0.65	PST-011-003	0.64
MCT-001-004	0.68	PST-020-001	0.66	PST-002-001	0.65	MCT-004-002	0.64
MST-002-002	0.68	PST-020-010	0.66	MCT-004-009	0.65	PST-020-007	0.64
PST-020-005	0.67	PST-004-011	0.66	PST-002-002	0.65	PST-020-013	0.64
PST-020-012	0.67	PST-004-005	0.66	PST-001-004	0.65	PST-011-002	0.64
PST-006-003	0.67	PST-004-003	0.66	PST-001-003	0.65	PST-003-008	0.64
PST-006-002	0.67	PST-020-003	0.66	PST-001-005	0.65	PST-003-007	0.64
PST-006-001	0.67	PST-004-004	0.66	PST-001-006	0.65	PST-011-001	0.64
MST-007-004	0.67	PST-020-004	0.66	MCT-004-006	0.65	MCT-004-004	0.64
PST-020-006	0.67	PST-020-011	0.66	MCT-004-011	0.65	PST-011-004	0.64
PST-005-005	0.66	PST-004-002	0.66	PST-002-006	0.65	PST-020-014	0.64
PST-005-004	0.66	PST-004-001	0.66	PST-002-007	0.65	MST-007-006	0.64
PST-005-006	0.66	MST-007-005	0.66	PST-002-003	0.65	MCT-004-001	0.63
PST-005-009	0.66	PST-011-010	0.66	PST-007-002	0.65	PST-011-005	0.63
PST-005-003	0.66	PST-003-004	0.66	PST-007-003	0.65	MCT-002-005S	0.63
PST-005-002	0.66	PST-003-005	0.66	PST-001-002	0.65	MST-007-007	0.63
PST-005-008	0.66	PST-003-003	0.66	PST-001-001	0.65	MCT-002-001S	0.63
PST-004-010	0.66	PST-003-006	0.66	MCT-004-008	0.64	MCT-002-003S	0.62

Figure D-1 is the trending analysis plot generated by the USLSTATS program with no additional administrative margin.

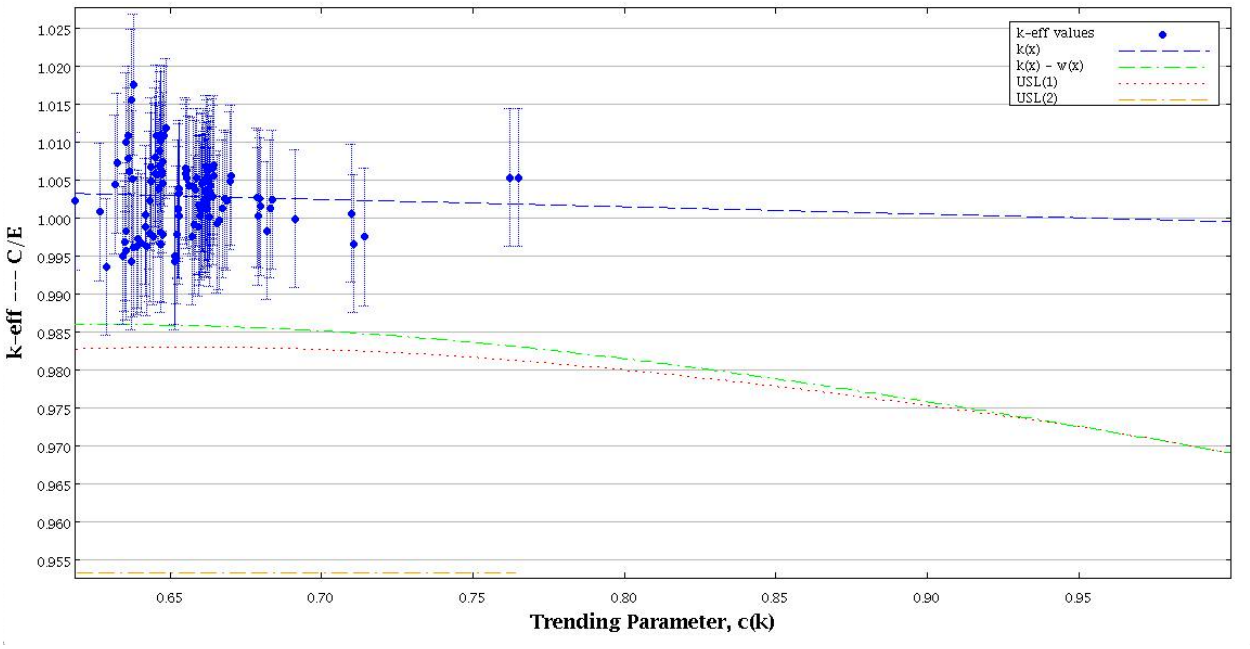

Figure D-1. Trending analysis plot of c(k) for reconfigured dry scenario.

The critical experiments used for benchmarking include, to the extent possible, configurations having neutronics and geometric characteristics comparable to those of the proposed design basis configurations. Because the application models are slightly outside the range of applicability of the benchmark experiments, as indicated by the c(k) values being less than optimal, an administrative margin of 0.02 is added to account for deficiencies in matching the critical experiments used for validation with the bounding models for this analysis. An additional margin is added to account for the potential bias from beryllium and chlorine, determined as described above using the uncertainty data for the beryllium and chlorine reactions from the sensitivity file. The respective numbers used to determine the USL along with the resultant USL are listed below:

Bias (from USLSTATS):	0.0010
Uncertainty in the bias (from USLSTATS):	0.0294
Margin for beryllium and chlorine:	0.0010
Administrative margin:	0.02
Resulting USL:	0.9486

D.2 RECONFIGURED WET SCENARIO

For the reconfigured wet scenario, the case chosen is g380infgenhx0200b050rd20vdfcbo, which has 50 g of B_4C and 545 g of beryllium into the waste form with a k_{eff} + 2σ of 0.79499 and an EALF of 0.39 eV. The case is an infinite flooded (with brine) array with full radial and vertical compaction. The TSUNAMI-IP calculated c(k) values are given in Table D-2. From the compared critical experiments, the c(k) values ranged from 0.63 to 0.78 Ideally, benchmark experiments should have a c(k) greater than 0.8 to be considered for validation. However, experiments that model materials similar to this waste form do not exist.

Table D-2. Reconfigured wet scenario c(k) values.

Experiment	c(k) value	Experiment	c(k) value	Experiment	c(k) value	Experiment	c(k) value
MCT-002-004S	0.78	PST-004-009	0.68	PST-003-006	0.67	MCT-004-003	0.66
MCT-002-006S	0.78	PST-004-010	0.68	PST-011-008	0.67	MCT-004-007	0.66
MST-007-002	0.73	MST-007-004	0.68	PST-011-011	0.67	PST-007-005	0.66
MST-007-001	0.72	PST-005-007	0.68	PST-011-009	0.67	PST-007-004	0.66
MCT-001-001	0.72	PST-004-008	0.68	MST-007-005	0.67	PST-007-002	0.65
MCT-001-002	0.70	PST-004-012	0.68	PST-011-006	0.67	PST-007-008	0.65
MST-002-003	0.70	PST-004-013	0.68	PST-003-002	0.67	MCT-004-005	0.65
MST-002-001	0.70	PST-020-002	0.68	PST-003-001	0.67	PST-020-008	0.65
MST-002-002	0.70	PST-004-006	0.68	MCT-004-009	0.66	PST-007-007	0.65
MST-007-003	0.69	PST-020-009	0.68	MCT-004-011	0.66	PST-007-006	0.65
MCT-001-003	0.69	PST-020-015	0.68	MCT-004-006	0.66	PST-011-003	0.65
MCT-001-004	0.69	PST-020-010	0.68	PST-002-001	0.66	PST-003-008	0.65
MCT-002-002S	0.69	PST-004-005	0.68	PST-002-005	0.66	PST-011-002	0.65
PST-006-003	0.68	PST-004-003	0.67	PST-002-002	0.66	PST-003-007	0.65
PST-006-002	0.68	PST-020-001	0.67	PST-002-004	0.66	PST-020-013	0.65
PST-006-001	0.68	PST-004-004	0.67	MCT-004-008	0.66	MCT-004-002	0.65
PST-020-005	0.68	PST-020-003	0.67	MCT-004-010	0.66	PST-011-001	0.65
PST-020-012	0.68	PST-004-011	0.67	PST-002-003	0.66	PST-011-004	0.65
PST-020-006	0.68	PST-004-002	0.67	PST-002-006	0.66	PST-020-007	0.65
PST-005-004	0.68	PST-004-001	0.67	PST-002-007	0.66	MCT-004-004	0.65
PST-005-005	0.68	PST-011-010	0.67	PST-007-001	0.66	PST-020-014	0.65
PST-005-009	0.68	PST-020-004	0.67	PST-001-003	0.66	MCT-004-001	0.65
PST-005-006	0.68	PST-020-011	0.67	PST-001-004	0.66	PST-011-005	0.65
PST-005-002	0.68	PST-003-004	0.67	PST-001-005	0.66	MCT-002-005S	0.65
PST-005-003	0.68	PST-003-003	0.67	PST-001-006	0.66	MST-007-006	0.65
PST-005-008	0.68	PST-011-012	0.67	PST-001-001	0.66	MST-007-007	0.64
PST-005-001	0.68	PST-003-005	0.67	PST-007-003	0.66	MCT-002-001S	0.64
PST-004-007	0.68	PST-011-007	0.67	PST-001-002	0.66	MCT-002-003S	0.63
PST-004-007	0.68	PST-011-007	0.67	PST-001-002	0.66	MCT-002-003S	0.63

Figure D-2 is the trending analysis plot generated by the USLSTATS program with no additional administrative margin.

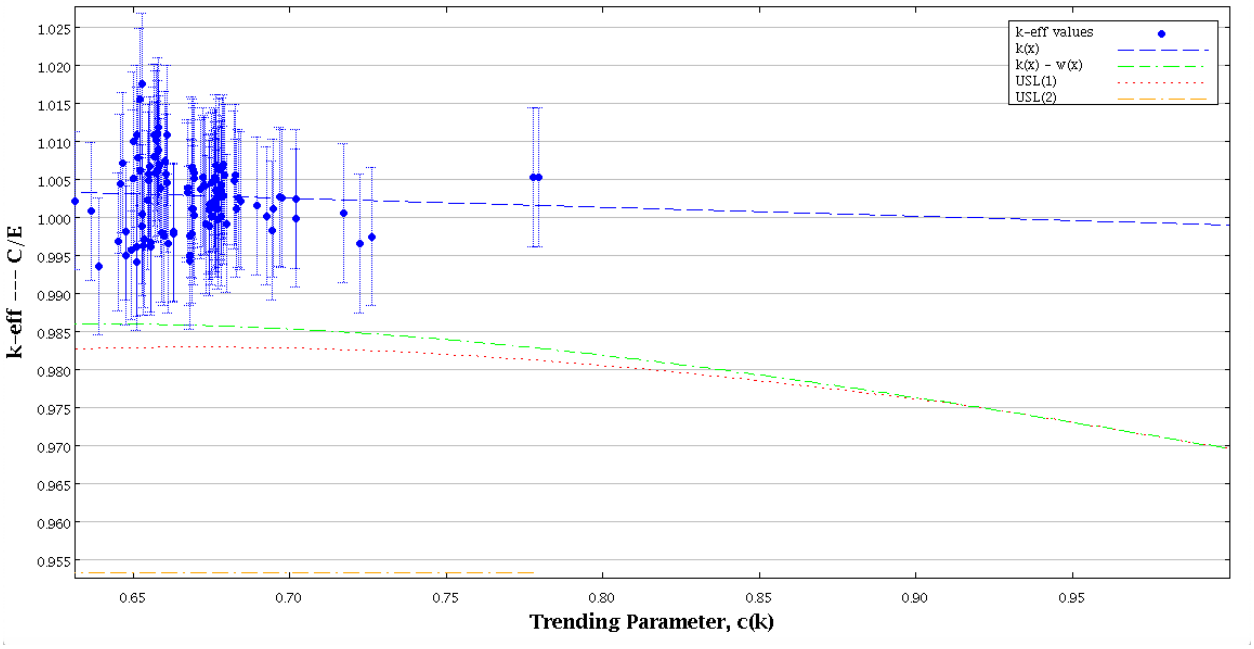

Figure D-2. Trending analysis plot of c(k) for reconfigured wet scenario.

The critical experiments used for benchmarking include, to the extent possible, configurations having neutronics and geometric characteristics comparable to those of the proposed design basis configurations. Because the application models are slightly outside the range of applicability of the benchmark experiments, as indicated by the c(k) values being less than optimal, an administrative margin of 0.02 is added to account for deficiencies in matching the critical experiments used for validation with the bounding models for this analysis. An additional margin is added to account for the potential bias from beryllium and chlorine, determined using the uncertainty data for the beryllium and chlorine reactions from the sensitivity file. The respective numbers used to determine the USL along with the resultant USL are listed below:

Bias (from USLSTATS):	0.0005
Uncertainty in the bias (from USLSTATS):	0.0305
Margin for beryllium and chlorine:	0.0014
Administrative margin:	0.02
Resulting USL:	0.9476

D.3 USING EALF FOR VALIDATION

For comparison, EALFs were also used as a trending parameter in USLSTATS, with the same 112 benchmarks. The benchmarks have EALFs ranging from 0.04 to 0.95 and are listed in Table D-3. Appendix B lists all the evaluation case results, including the respective EALFs, with the bounding cases in each table bolded. For cases having 50 g B_4C or less, the EALFs range from 0.05 to 1.52 eV (including both dry and wet scenarios).

Table D-3. Dry mixed container array with minimum credited spacing c(k) values.

Experiment	EALF value	Experiment	EALF value	Experiment	EALF value	Experiment	EALF value
MCT-001-001	0.95	MCT-001-004	0.11	PST-002-002	0.07	PST-011-011	0.06
MCT-002-002S	0.72	PST-007-006	0.11	PST-002-001	0.07	PST-005-009	0.06
MCT-002-001S	0.54	PST-007-007	0.11	PST-003-006	0.07	PST-005-003	0.06
PST-001-006	0.34	PST-007-004	0.11	PST-005-007	0.07	PST-005-008	0.06
MCT-002-004S	0.27	PST-007-005	0.11	PST-004-011	0.07	PST-005-002	0.06
MCT-001-002	0.27	PST-007-003	0.11	PST-011-004	0.07	PST-004-008	0.06
PST-007-001	0.27	PST-001-002	0.11	PST-011-003	0.07	PST-004-004	0.06
PST-007-002	0.25	PST-020-014	0.10	PST-005-006	0.07	PST-004-007	0.06
MCT-002-003S	0.19	PST-007-008	0.10	PST-020-001	0.06	PST-004-012	0.06
MST-007-007	0.18	PST-020-007	0.10	PST-003-005	0.06	PST-004-013	0.06
MCT-002-006S	0.18	PST-002-007	0.10	PST-020-009	0.06	PST-005-001	0.06
MST-007-006	0.18	MCT-004-007	0.09	PST-020-002	0.06	PST-006-003	0.05
MCT-001-003	0.16	PST-002-006	0.09	PST-011-002	0.06	PST-011-010	0.05
MST-007-005	0.16	MCT-004-008	0.09	PST-004-010	0.06	PST-004-006	0.05
PST-001-005	0.16	MCT-004-009	0.09	PST-005-005	0.06	PST-004-003	0.05
MST-007-004	0.15	PST-001-001	0.09	PST-011-001	0.06	PST-004-005	0.05
PST-001-004	0.15	PST-002-005	0.08	PST-003-004	0.06	PST-004-002	0.05
MST-007-003	0.15	PST-002-004	0.08	PST-003-003	0.06	PST-011-012	0.05
MCT-004-001	0.14	MCT-004-010	0.08	PST-020-006	0.06	PST-006-002	0.05
MCT-004-002	0.14	MCT-004-011	0.08	PST-003-008	0.06	PST-004-001	0.05
MCT-004-003	0.14	PST-020-012	0.08	PST-005-004	0.06	PST-011-009	0.05
MCT-002-005S	0.14	PST-020-005	0.08	PST-003-002	0.06	PST-006-001	0.05
PST-001-003	0.13	PST-002-003	0.08	PST-003-007	0.06	PST-011-007	0.05
MST-007-002	0.13	PST-020-004	0.08	PST-020-003	0.06	PST-011-008	0.05
MCT-004-004	0.12	PST-020-013	0.08	PST-020-010	0.06	PST-011-006	0.05
MST-007-001	0.12	PST-020-008	0.08	PST-004-009	0.06	MST-002-003	0.04
MCT-004-005	0.12	PST-020-011	0.07	PST-020-015	0.06	MST-002-001	0.04
MCT-004-006	0.12	PST-011-005	0.07	PST-003-001	0.06	MST-002-002	0.04

Figure D-3 is the trending analysis plot generated by the USLSTATS program with no additional administrative margin.

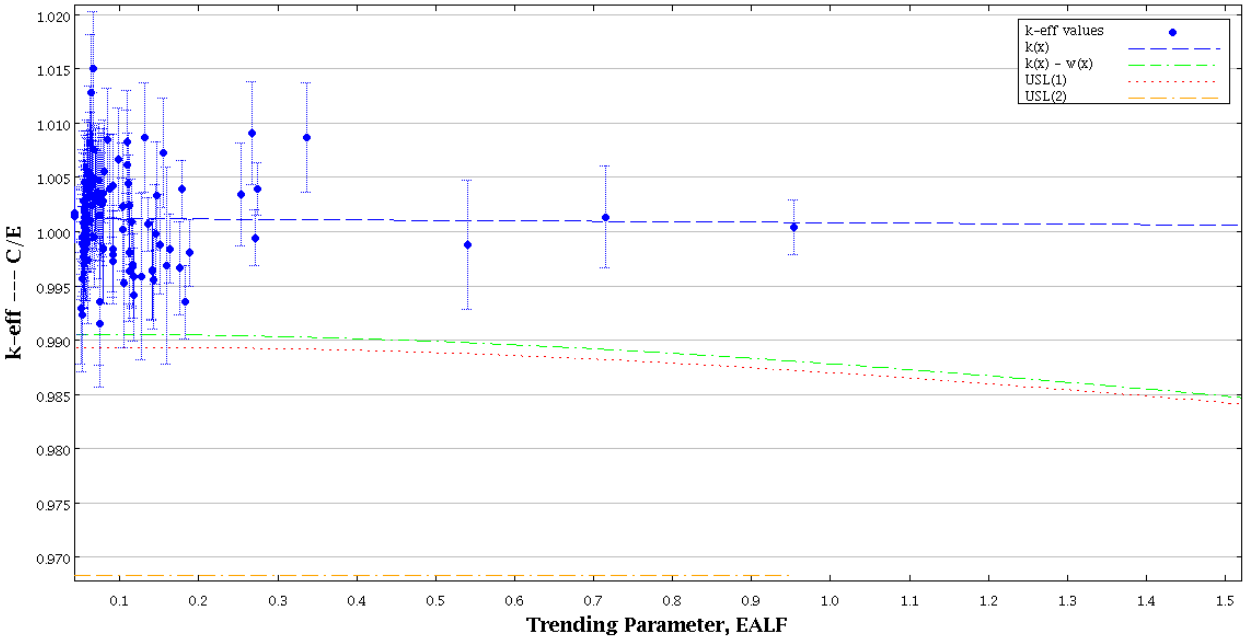

Figure D-3. Trending analysis plot using EALF values.

A majority of the EALFs are below the range of evaluation case EALFs. To account for those outside the range, an administrative margin of 0.02 is added to account for deficiencies in matching the critical experiments used for validation with the bounding models for this analysis. The respective numbers used to determine the USL along with the resultant USL are listed below (bounding values used).

Bias (from USLSTATS):	0.0000 (set to zero since it is positive)
Uncertainty in the bias (from USLSTATS):	0.0159
Administrative margin:	0.02
Resulting USL:	0.9641

D.4 SUMMARY OF USLS

Table D-4 lists the respective scenarios, their respective biases (positive biases set to zero), bias uncertainties from USLSTATS, additional administrative margin, and the calculated USLs. As illustrated, they both result in comparable biases. The critical experiments used for benchmarking included, to the extent possible, configurations having neutronics and geometric characteristics comparable to those of the proposed design basis configurations. Because the application models are slightly outside the range of applicability of the benchmark experiments, an administrative margin of 0.02 has been applied to determine final USLs. This additional margin accounts for deficiencies in matching the critical experiments used for validation with the bounding models for this analysis.

Table D-4. USL summary.

Scenario	Bias based on c(k)*	Bias uncertainty	Bias for beryllium and chlorine	Administrative margin	USL
Dry reconfigured	0.0010	0.0294	0.0010	0.02	0.9486
Wet reconfigured	0.0005	0.0305	0.0014	0.02	0.9476
Scenario	**Bias based on EALF***	**Bias uncertainty**	**Bias for beryllium and chlorine**	**Administrative margin**	**USL**
All	0.0000	0.0159	NA	0.02	0.9641

*Positive bias set to 0

Based on the conservative USLs determined with c(k) trending, any dry scenario result ($k_{eff} + 2\sigma$) less than 0.9486 and any wet scenario result less than 0.9476 can be considered to be subcritical.

D.5 REFERENCES

[1] American National Standards Institute (ANSI). 2014. *An American National Standard for Nuclear Criticality Safety in Operations with Fissionable Materials Outside Reactors*, ANSI/ANS-8.1-2014, La Grange Park, IL: American National Standards Institute, Inc.

[2] ANSI. 2017. *An American National Standard for Validation on Neutron Transport Methods for Nuclear Criticality Safety Calculations*, ANSI/ANS-8.24-2017, La Grange Park, IL: American National Standards Institute, Inc.

[3] Nuclear Energy Agency (NEA). 2016. *International Handbook of Evaluated Criticality Safety Benchmark Experiments,* NEA/NSC/DOC(95)03, NEA Nuclear Science Committee.

[4] ORNL. 2013. *The SCALE Verified, Archived Library of Inputs and Data – VALID*, Oak Ridge National Laboratory, transactions of ANS NCSD 2013, Wilmington, NC, September 29 – October 31, 2013.

[5] Nuclear Regulatory Commission (NRC). 2012. *An Approach for Validating Actinide and Fission Product Burnup Credit Criticality Safety Analyses-Criticality (k_{eff}) Predictions*, US Nuclear Regulatory Commission, NUREG/CR-7109, Oak Ridge National Laboratory, Oak Ridge, Tennessee.